

# S-conical minimal surfaces.

## Towards a unified theory of discrete minimal surfaces.

Alexander I. Bobenko, Benno König, Tim Hoffmann, and Stefan Sechelmann\*

November 12, 2015

### 1 Introduction

The theory of discrete minimal nets is an ongoing subject of investigation. The variety of approaches reaches from area variation of triangle meshes [PP93] to various versions of integrable discretizations – in particular as circular [BP96, BP99], s-isothermic [BHS06], and conical nets [LPW<sup>+</sup>06]. Recent developments show that these different approaches have more in common than previously thought [WYL15]. In this paper we show that a particular class of conical minimal nets possess a theory that is very similar to the one of s-isothermic minimal nets detailed in [BHS06] and that indeed the two classes of minimal nets are tightly linked through their respective associated families.

The integrable systems approach to (discrete) minimal surfaces relies on the fact that minimal surfaces are isothermic surfaces and thus possess conformal curvature line parametrizations. In fact minimal surfaces can be characterized as isothermic surfaces that have their Gauss map as dual. Discrete nets that are dualizable are called Koenigs nets [BS09] and the circular, s-isothermic and conical variants of minimal nets differ by what version of discrete curvature line parametrization is combined with this dualizability.

The paper is organized as follows: after collecting the basic definitions of conical nets and their curvature theory as given by the discrete Steiner’s formula [BPW10] (see also [BS08]) we recall the notion of Koenigs nets as discrete nets that are dualizable and introduce the notion of s-conical minimal surface by means of their Gauss map. In section 6 we describe how to construct these minimal nets given the combinatorial data of the conformal curvature lines on the desired surfaces. Section 7 we provide discrete analogs of some of the classical minimal surfaces. The associated family for s-conical minimal surfaces is introduced in section 8. A discrete version of the classical Weierstrass representation of minimal surfaces is given in section 9. Finally the connection between s-conical minimal surfaces and s-isothermic minimal nets is detailed in section 10. We close with an appendix on the construction of general conical minimal nets.

---

\*This research was supported by the DFG-Collaborative Research Center, TRR 109, “Discretization in Geometry and Dynamics”

## 2 Conical nets

In this paper we investigate conical nets that are minimal in the sense that a particular definition of mean curvature vanishes. Conical nets as defined below are Q-nets, which in turn are discrete surfaces with planar quadrilateral faces. Whenever we investigate local theory, one can think of the nets as having the combinatorics of the square grid  $f : \mathbb{Z}^2 \rightarrow \mathbb{R}^3$ . In general however, they have combinatorics  $f : V(D) \rightarrow \mathbb{R}^3$ , where  $V(D)$  is the vertex set of a quad-graph  $G$ . The latter is a strongly regular cell decomposition of a two-dimensional manifold with all faces being quadrilaterals. Moreover in the developed theory of discrete CMC surfaces the quad-graph should be edge-bipartite, i.e. there is a black and white edge coloring such that for each quadrilateral opposite edges are of the same color.

In what follows we will use a notation that indicates shifts in the various directions by subscript. For a net  $f : \mathbb{Z}^2 \rightarrow \mathbb{R}^3$  we will denote a generic point  $f(k, l)$  simply by  $f$ . Then it is understood that  $f_1 = f(k+1, l)$ ,  $f_2 = f(k, l+1)$ ,  $f_{12} = f(k+1, l+1)$ ,  $f_{\bar{1}} = f(k-1, l)$  and so forth. This is of particular use in case of  $\mathbb{Z}^n$  lattices but also as long as only one or two neighboring quadrilaterals of a quad-graph are concerned it is a useful shorthand. The following definition first appeared in [LPW<sup>+</sup>06].

**Definition 1.** A *conical net* is a Q-net in  $\mathbb{R}^3$  such that all faces incident with a vertex are in oriented contact with a cone of revolution originating in that vertex.

Equivalently one can require the faces incident with a vertex to be in oriented contact with a common sphere. That sphere will not be unique but the centers of all touching spheres will lie on the axis of the cone.

The properties of conical nets mentioned in this section are due to [LPW<sup>+</sup>06] – see also [BS08, BPW10]:

Generically, the axis of that cone furnishes a unique normal at each vertex.<sup>1</sup> So a conical net  $f : V(D) \rightarrow \mathbb{R}^3$  comes with two sets of canonical normals: A face normal  $N : F(D) \rightarrow S^2$ ,  $F(D)$  denoting the faces of  $G$ , and a vertex normal.

**Theorem 1.** *Given a conical net  $f : V(D) \rightarrow \mathbb{R}^3$  one can consider the offset net  $f^t : V(D) \rightarrow \mathbb{R}^3$  given by moving each face of  $f$  by distance  $t$  in direction of the face normal  $N$ . Then  $f^t$  is a conical net by itself. Moreover,  $f$  and  $f^t$  have parallel edges.*

*Proof.* Obviously  $f^t$  is a Q-net. Furthermore at any given vertex the faces  $f$  incident with it touch a sphere  $s$  of radius say  $r$  around a center  $c$ . Then the corresponding faces of  $f^t$  touch a sphere of radius  $r + t$  around  $c$ . Thus,  $f^t$  is a conical net. Finally, The edges of  $f$  and  $f^t$  are parallel since corresponding faces incident with the edges lie in parallel planes.  $\square$

**Definition 2.** We will call the Q-net  $n := f^1 - f : V(D) \rightarrow \mathbb{R}^3$  the *(vertex) Gauss map* of  $f$ .  $n$  is again a conical net.

---

<sup>1</sup>There are situations where the normal is not well defined except for the plane (which has a canonical normal direction anyway) these situations can not appear for minimal nets as defined later on.

Note that the Gauss map  $n : V(D) \rightarrow \mathbb{R}^3$  is not of unit length. Also note that the Gauss map  $n$  and the nets  $f$  and  $f^t$  all have parallel edges  $f_i - f \parallel f_i^t - f^t \parallel n_i - n$ ,  $i \in \{1, 2\}$  since again the corresponding faces incident with the edges lie in parallel planes.

The following is a direct consequence of the definition of the face and vertex normals:

**Lemma 2.** *Let  $f : V(D) \rightarrow \mathbb{R}^3$  be a conical net with face normals  $N$  and vertex normals  $n$ . Then  $N : F(D) \rightarrow S^2$  furnishes a circular  $Q$ -net and  $n : V(D) \rightarrow \mathbb{R}^3$  is a  $Q$ -net with faces tangent to  $S^2$ .*

### 3 Steiner's formula, curvatures, and minimal nets

For smooth immersions  $f$  in  $\mathbb{R}^3$  Steiner's formula is an equation that couples the areas of the surface  $f$  and a parallel offset surface  $f^t$  with the mean and Gauss curvature of  $f$ . In particular if  $f$  is an infinitesimal surface patch and  $f^t$  a parallel one in distance  $t$  in normal direction, then Steiner's formula yields

$$A(f^t) = A(f)(1 - 2Ht + Kt^2) \quad (1)$$

where  $A$  denotes the area,  $H$  and  $K$  are the mean curvature and the Gauss curvature of  $f$ .

In [BPW10] a discrete analogue of this formula was introduced that allows to define curvatures for  $Q$ -nets with a given Gauss map (see also [Sch03] where this formula first appeared for  $Q$ -nets with circular quadrilaterals). Let  $Q = (f, f_1, f_{12}, f_2)$  be a planar quadrilateral of  $f$  and  $N$  its unit face normal. Denoting its diagonals with  $d_1 = f_{12} - f$  and  $d_2 = f_2 - f_1$  the area  $A(Q)$  can be computed as<sup>2</sup>

$$A(Q) = \frac{1}{2} \det(d_1, d_2, N).$$

Now, if  $P$  is another quadrilateral with edges parallel to  $Q$  and with diagonals  $c_1$  and  $c_2$  the area of  $P + tQ$  can be found to be

$$A(P + tQ) = A(P) + 2t \frac{1}{4} (\det(d_1, c_2, N) + \det(c_1, d_2, N)) + t^2 A(Q) \quad (2)$$

Since the Gauss map of a conical net has parallel edges we have shown the following lemma:

**Lemma 3.** *Given a conical net  $f : V(D) \rightarrow \mathbb{R}^3$  and its Gauss map  $n : V(D) \rightarrow \mathbb{R}^3$  the quadrilaterals of the offset net  $f^t = f + t n$  have an area that is quadratic in the distance  $t$ .*

The linear term is to some extent a mixture of the areas of  $P$  and  $Q$  and is known under the name *mixed area*. The space of all planar quadrilaterals with edges parallel to a given one  $Q$  is a four dimensional vector space. Modding out the translations leaves a two dimensional one. On this space the area is a quadratic form  $A(P)$  and the mixed area is the corresponding symmetric form  $A(P_1, P_2)$ :

---

<sup>2</sup>The sign here depends on the choice of the normal  $N$ .

**Definition 3.** Let  $P = (p, p_1, p_{12}, p_2)$  and  $Q = (q, q_1, q_{12}, q_2)$  be two planar quadrilaterals with parallel edges and let  $N$  be their common normal then the *mixed area*  $A(P, Q)$  of  $P$  and  $Q$  is given by

$$A(P, Q) = \frac{1}{4} (\det(p_{12} - p, q_2 - q_1, N) + \det(q_{12} - q, p_1 - p_2, N)). \quad (3)$$

Note that  $A(Q, Q) = A(Q)$  holds. For a net  $f$  we will write  $A(f)$  for the area of the quadrilateral  $(f, f_1, f_{12}, f_2)$  and likewise for mixed areas.

Now we are in the position to define a discrete Steiner formula in the spirit of eq. 1 as proposed in [BPW10] (see also [BS08]):

**Definition 4.** Let  $f : V(D) \rightarrow \mathbb{R}^3$  be a Q-net and  $n : V(D) \rightarrow \mathbb{R}^3$  another one (considered the Gauss map of  $f$ ) with parallel edges. Then for each quadrilateral of  $f$  we define the *discrete mean curvature*  $H$  and the *discrete Gauss curvature*  $K$  by

$$A(f + tn) = A(f)(1 - 2Ht + Kt^2). \quad (4)$$

This equation is called *discrete Steiner formula* and one finds  $H = -\frac{A(f, n)}{A(f)}$  and  $K = \frac{A(n)}{A(f)}$ .

Since a conical net has a Gauss map  $n$  that has parallel edges we are now in the position to define conical minimal nets:

**Definition 5.** A Q-net  $f : V(D) \rightarrow \mathbb{R}^3$  is called *minimal* if it has vanishing mean curvature  $H$ .

The formula for the mean curvature implies that a conical net is minimal exactly if and only if  $A(f, n) = 0$  holds. Therefore we need to characterize pairs of nets such that for all quadrilaterals the mixed area vanishes.

## 4 Dual quadrilaterals and Koenigs nets

As mentioned above the space of all planar quadrilaterals with parallel edges up to translations is a two dimensional vector space and quadrilaterals  $P$  with  $A(P, Q) = 0$  are the ones that are “orthogonal” to  $Q$  with respect to the mixed area form on that space (see [BS08]). So for any non-vanishing planar quadrilateral  $P$  there is a  $Q$  with  $A(P, Q) = 0$  and  $Q$  is unique up to scaling.

**Definition 6.** Two planar quadrilaterals  $P$  and  $Q$  are called *dual* to each other if their mixed area vanishes:

$$A(P, Q) = 0.$$

Whenever scaling is unimportant we will simply talk about *the* dual of a planar quadrilateral  $P$  and denote it by  $P^*$ .

Here is a way to characterize dual quadrilaterals:



**Lemma 4.** Let  $P = (p, p_1, p_{12}, p_2)$  and  $Q = (q, q_1, q_{12}, q_2)$  be two planar quadrilaterals with parallel edges and let  $N$  be their common normal then the mixed area  $A(P, Q)$  of  $P$  and  $Q$  vanishes iff  $p_{12} - p \parallel q_2 - q_1$  and  $q_{12} - q \parallel p_2 - p_1$ .

The proof for this can be found for example in [BS08, BPW10]

We have seen above that any planar quadrilateral has a dual one. However, a Q-net as a whole does not need to be dualizable. There is an extra condition for the scaling of the dual quadrilaterals around a vertex to close up.

**Definition 7.** Let  $f : V(D) \rightarrow \mathbb{R}^3$  be a Q-net. If there is another Q-net  $f^* : V(D) \rightarrow \mathbb{R}^3$  such that corresponding quadrilaterals of  $f$  and  $f^*$  are dual to each other  $f$  is called a *Koenigs net* and  $f^*$  its (*Koenigs*) *dual*.

This notion was introduced in [BS09]. Being conical and Koenigs is compatible in the following sense:

**Lemma 5.** If  $f : V(D) \rightarrow \mathbb{R}^3$  is conical and Koenigs, its dual  $f^* : V(D) \rightarrow \mathbb{R}^3$  is conical as well.

*Proof.* The planes of a planar quadrilateral and its dual are parallel. Thus, the conicality condition for  $f^*$  holds iff it holds for  $f$ .  $\square$

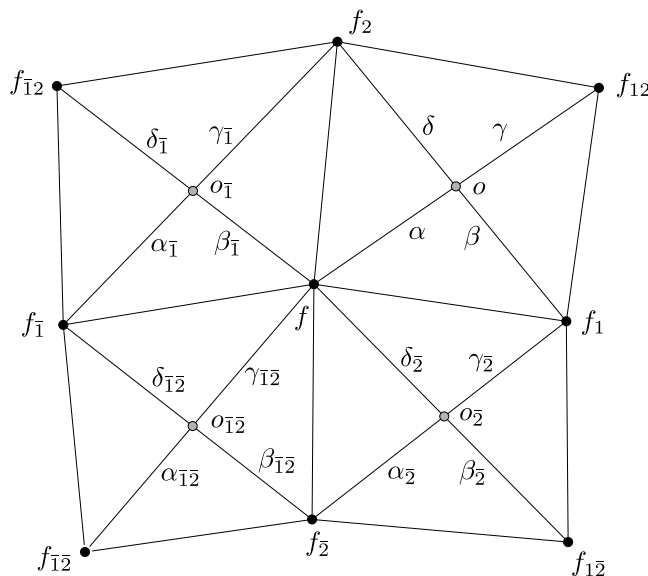


Figure 1: The condition for a net to be Koenigs.

There are various ways to characterize Koenigs nets (see again [BS08]). Using the labeling in figure 1 the most general is

$$1 = \frac{\alpha \delta}{\beta_1 \gamma_1} \frac{\beta_1 \alpha_1}{\delta_{12} \gamma_{12}} \frac{\beta_{12} \gamma_{12}}{\delta_2 \alpha_2} \frac{\delta_2 \gamma_2}{\alpha \beta} = \frac{\delta \alpha_1 \beta_{12} \gamma_2}{\gamma_1 \delta_{12} \alpha_2 \beta}. \quad (5)$$

This condition is necessary and on a simply connected quad-graph sufficient for a O-net to be Koenigs (see [BS08]). The following geometric condition characterizes Koenigs nets on  $\mathbb{Z}^2$  combinatorics: Given a Q-net  $f : V(D) \rightarrow \mathbb{R}^3$  the diagonals in each quadrilateral do intersect. We will denote these points by  $o$ .

**Lemma 6.** *If  $f : V(D) \rightarrow \mathbb{R}^3$  is a Q-net in general position (each vertex and its neighbours are not co-planar) and if the diagonal intersections  $o$  form planar faces around each vertex as well then  $f$  is a Koenigs net.*

For a proof once again see [BS08].

## 5 conical minimal nets and Koebe polyhedra

Now we are able to characterize conical minimal nets as particular Koenigs nets namely Koenigs nets  $f : V(D) \rightarrow \mathbb{R}^3$  that have their Gauss map  $n : V(D) \rightarrow \mathbb{R}^3$  as a dual.

Conical nets possess the property that they come with a 2-parameter family of circular nets i.e. Q-nets with circular faces. This can be seen as follows: Given a conical net one can choose a point on one of the face's planes arbitrarily. Mirroring this point at the planes spanned by the face's edges and their incident vertex normals gives a circular net. Each vertex of this circular net corresponds to a face of the conical net and vice versa. This way each conical net gives rise to a 2-parameter family of circular nets. The circle centers of the circular net lie on the cone axes of the conical one.

Now for a conical Koenigs net we have the planar net of diagonal intersections  $o : F(D) \rightarrow \mathbb{R}^3$  for valence 4 vertices and we will restrict ourselves to the natural case where the net of diagonal intersections is circular in the above way.

**Definition 8.** An *s-conical Gauss map* is a Q-net  $n : V(D) \rightarrow \mathbb{R}^3$  (with convex faces) such that each face touches the unit sphere in its diagonal intersection point.

The definition ensures that the diagonal intersections are circular and that they coincide with the face normals  $N$ . The circle is the orthogonal intersection of a sphere around the vertex with the unit sphere (see fig. 2). The faces are also tangent to the cone through this circle with tip at the vertex. Cf. [BS08, Theorem 3.21].

**Lemma 7.** *The diagonals of the quadrilaterals in an s-conical Gauss map intersect at a constant angle  $\sigma$ .*

*Proof.* Each edge connects the centers of two spheres on which both the diagonal intersection points of the adjacent quadrilaterals lie, so both diagonal intersection angles are equal to the intersection angle of the spheres.  $\square$

**Proposition 8.** *S-conical Gauss maps on a simply connected domain with even valency at all interior vertices are Koenigs nets.*

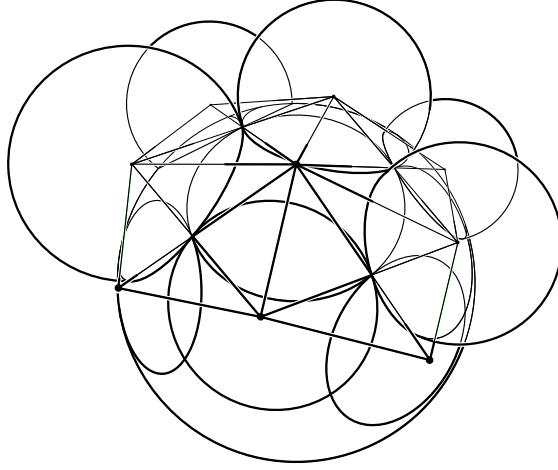


Figure 2: Some quadrilaterals of an  $s$ -conical Gauss map with diagonals, the circles, and some of the spheres around the vertices

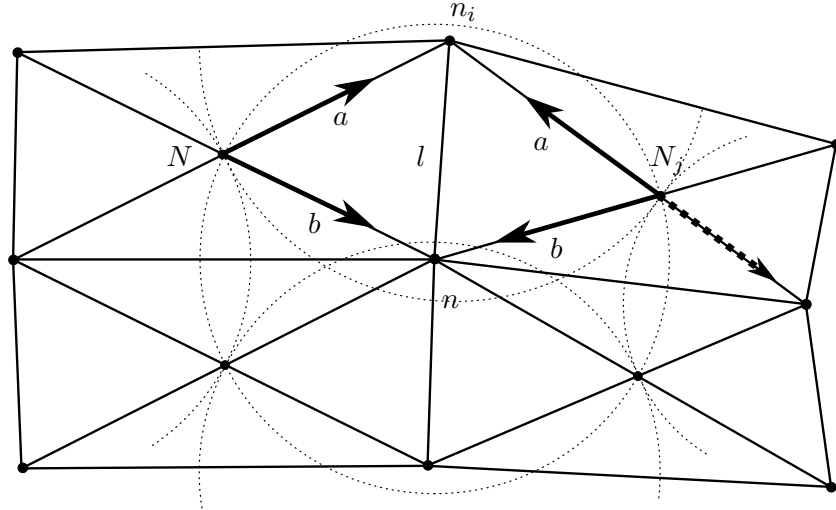


Figure 3: Four quadrilaterals depicting a situation equivalent to proposition 8 in the plane.

*Proof.* Recall that in the standard construction (cf. [BS08, p. 48]) of a dual quadrilateral the length  $l^*$  of the dual edge corresponding to an edge with length  $l$  is  $l^* = \frac{1}{ab}l$ , with  $a$  and  $b$  the lengths of the diagonal segments connecting the intersection point to the two vertices of the edge. In our case, the diagonal intersection points of two quadrilaterals sharing an edge  $n_i - n$  are the face normals  $N, N_j$  and lie on spheres around  $n$  and  $n_i$ , thus the diagonal segment lengths on both sides of the edge coincide. So without rescaling the dual quadrilaterals fit together up to a factor of  $\pm 1$ .

The construction of duals involved choosing two diagonal direction unit vectors; an edge retained its orientation precisely if the signs of its vertices (with the diagonal

intersection point assumed to be 0) with respect to this choice coincided. So going around a vertex of  $n$ , the adjacent edges alternate between retaining and reversing orientation. An even number of edges results in simultaneous dualizability of all adjacent quadrilaterals.  $\square$

**Definition 9.** The dual  $f$  of an  $s$ -conical Gauss map  $n$  is conical minimal. We will call these nets *s-conical minimal surface*.

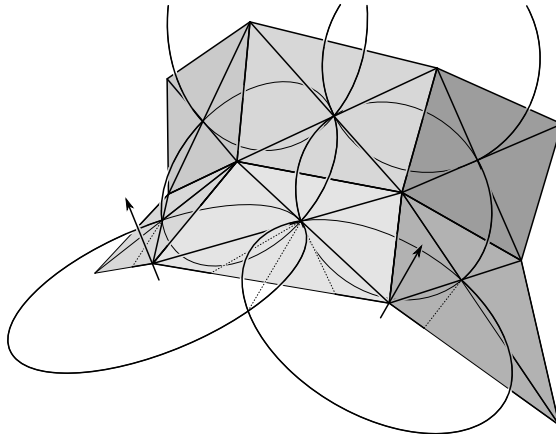


Figure 4: Some quadrilaterals of an  $s$ -conical minimal surface with diagonals and the circles which arise as intersections of the spheres around vertices and the planes containing the diagonal intersections

Since  $f$  is edge-parallel to  $n$  by definition of duality, it shares the face normals  $N$ . The faces adjacent to each vertex are still tangent to cones with tip at the vertex  $f$  and axis parallel to  $n$ . So  $n$  is indeed a vertex Gauss map for  $f$ .

Figure 4 shows some quadrilaterals of a  $s$ -conical minimal surface with vertex normals and the circular intersection points of the diagonals.

We defined  $s$ -conical minimal surfaces by means of their Gauss maps. This shifts questions of existence and uniqueness to likewise questions for the Gauss map. Quad-graphs  $D$  are known to arise as the combination of a cell decomposition  $\Gamma$  together with its dual decomposition  $\Gamma^*$ . Following [BHS06] we quote the following two theorems:

**Theorem 9.** *For every polytopal cellular decomposition of the sphere, there exists a pattern of circles in the sphere with the following properties. There is a circle corresponding to each face and to each vertex. The vertex circles form a packing with two circles touching if and only if the corresponding vertices are adjacent. Likewise, the face circles form a packing with circles touching if and only if the corresponding faces are adjacent. For each edge, there is a pair of touching vertex circles and a pair of touching face circles. These pairs touch in the same point, intersecting each other orthogonally. This circle pattern is unique up to Möbius transformations.*

This theorem was first stated and proved in [BS93]. Generalizations can be found in [Sch92], [Riv96], and [BS03]. See the latter in particular for a variational proof.

**Theorem 10.** *Every polytopal cellular decomposition of the sphere can be realized by a polyhedron with edges tangent to the sphere. This realization is unique up to projective transformations which fix the sphere. There is a simultaneous realization of the dual polyhedron, such that corresponding edges of the dual and the original polyhedron touch the sphere in the same points and intersect orthogonally.*

**Definition 10.** The polyhedra that arise by the above theorem are called *Koebe polyhedra*. We will call the polyhedron that arises from vertices of a Koebe polyhedron and its dual (and thus realizes the quad graph associated to the cellular decompositions  $\Gamma$  and  $\Gamma^*$ ) *circumscribed Koebe polyhedra*.

*Remark.* Note that the faces of a circumscribed Koebe polyhedra do touch the sphere in the intersection of the edges of the two dual Koebe polyhedra (hence the name): Given two neighboring vertices  $a$  and  $c$  of a Koebe polyhedron, their common edge touches the  $S^2$  in a point  $p$ . The two incident faces have inscribed circles  $c_b$  and  $c_d$  touching the edge at  $p$ . Let  $b$  and  $d$  denote the tips of the cones that touch  $S^2$  in the two circles  $c_b$  and  $c_d$ . Then  $b$  and  $d$  are the incident vertices of the dual Koebe polyhedron and the line connecting  $b$  and  $d$  is an edge of that and thus tangent to  $S^2$  as well. Moreover it is perpendicular to the circles  $c_b$  and  $c_d$  and thus perpendicular to the edge  $ac$ . Hence, the quadrilateral  $a, b, c, d$  is planar, tangent to  $S^2$  and has diagonal that are perpendicular and that intersect in the touching point.

This in particular shows:

**Proposition 11.** *Circumscribed Koebe polyhedra give rise to  $s$ -conical Gauss maps.*

*Proof.* This is clear if the (inner) vertices have even valence. Vertices with odd valence can be treated as branch points and the polyhedron then is treated as a branched cover.  $\square$

*Remark.* Later we will use the notion of circumscribed Koebe polyhedra in a rather lax way meaning not only polyhedra but more general polyhedral surfaces with perpendicular diagonals and all faces touching  $S^2$  in their diagonal intersection points.

**Definition 11.** We will call a quad-graph  $D$  *admissible* iff its corresponding cell decomposition  $\Gamma$  is realizable as an orthogonal circle pattern.

**Theorem 12.** *Given an admissible quad-graph  $D$ . Then there is a  $s$ -conical minimal surface  $f : V(D) \rightarrow \mathbb{R}^3$ . In particular, if  $D$  arises from a topological cell decomposition of the 2-sphere then  $f$  is unique up to Möbius transformations.*

*Proof.* Given an admissible quad-graph  $D$ , we know that there is a realization as a circle pattern in  $S^2$ . This gives rise to a circumscribed Koebe polyhedron of the same combinatorics. Possibly treating it as a branched cover, this furnishes an  $s$ -conical Gauss map by Proposition 11. By definition its dual then is an  $s$ -conical minimal surface. The uniqueness in case of a cell decomposition of the sphere follows from Theorem 9.  $\square$

*Remark.* Note that the S-conical Gauss maps that arise this way have perpendicular diagonals as they arise from the orthogonality of the underlying circle pattern. There is a known associated family for these circle patterns that generalizes them to patterns with circle pattern angle  $\sigma \neq \pi/2$  (see [BS08]). The patterns of fixed angle give rise to S-conical Gauss maps as well, albeit not orthogonal ones.

## 6 Construction of s-conical minimal surfaces

We will now briefly discuss how to find s-conical analogs of given minimal surfaces. The quad-graphs we are considering arise from cellular decompositions of 2-dim manifolds possibly with boundary.

1. *Discretize the Gauss map.* Recall, that conformal curvature lines on a surface can be thought of as a net of infinitesimal squares. The first step is finding a finite equivalent of that. Only its combinatorics matter. Again it is easier to work with the Gauß map. The Gauss map of the surface maps the curvature lines conformally to (a branched cover of) the sphere. In parameter space choose an evenly spaced grid of curvature lines. This defines the combinatorics of the discrete Gauss map. While the spacing of the lattice reflects the level of refinement the exceptional vertices correspond to umbilics and ends of the surface.

2. *Orthogonal circle pattern.* Next the orthogonal circle pattern corresponding to this polyhedral cell decomposition of the (branched cover of the) sphere needs to be constructed. This is generally done by finding critical points of the following spherical functional (for full details see [BHS06]) expressed in the the variables  $\rho_i = \log \tan \frac{r_i}{2}$  given by the spherical radii  $r_i$ :

$$S(\rho) = \sum_{(j,k)} (\operatorname{Im} \operatorname{Li}_2(i e^{\rho_k - \rho_j}) + \operatorname{Im} \operatorname{Li}_2(i e^{\rho_j - \rho_k}) - \operatorname{Im} \operatorname{Li}_2(i e^{\rho_j + \rho_k}) - \operatorname{Im} \operatorname{Li}_2(i e^{-\rho_j - \rho_k}) \\ - \pi(\rho_j + \rho_k)) + \sum_j \Phi_j \rho_j.$$

Here, the first sum is taken over all pairs  $(j, k)$  of neighboring circles and the second one runs over all circles  $j$ . The dilogarithm function  $\operatorname{Li}_2(z)$  is defined by  $\operatorname{Li}_2(z) = -\int_0^z \log(1-\zeta) d\zeta/\zeta$ . For each circle  $j$ ,  $\Phi_j$  gives the angle that is covered by its neighboring circles. It is normally  $2\pi$  for interior circles, but it differs for circles on the boundary and for circles where the pattern branches.

In many cases (in particular in case of unbranched cellular decompositions of the sphere) the circle radii can be obtained by minimizing the analogous euclidean functional [BS03] that is known to be convex. In some cases (see Enneper and Helicoid examples) the circle pattern can even be given explicitly.

Once the radii are known the circles can be laid out. The still remaining freedom of applying a Möbius transformation can be fixed (up to a simple rotation) by requiring the center of mass to be at the sphere center. Other normalizations – like fixing the position of some vertices that correspond to given normals – are of course possible and needed sometimes.

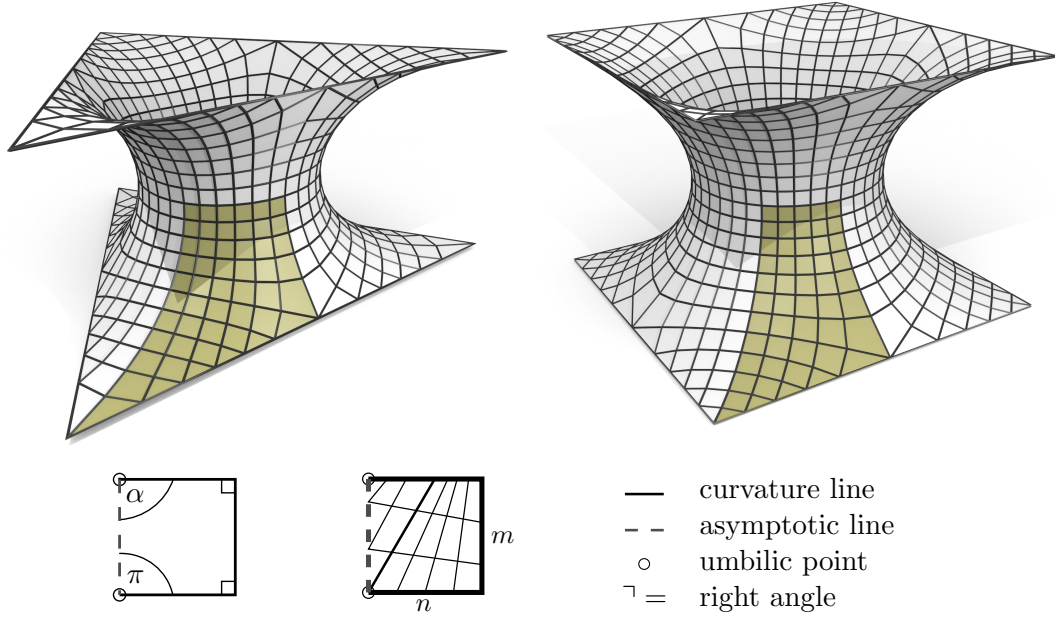


Figure 5: S-conical Schwarz H surface (top left) and fundamental piece (hi-lighted),  $\alpha = \pi/3$ . Combinatorial picture of the boundary conditions on  $\mathbb{S}^2$  and curvature line parametrization of fundamental piece of the Gauss image (bottom). S-conical Schoen I6 surface (top right),  $\alpha = \pi/4$ . Note that the nets are rotated to show their similarity, not edge parallelity.

3. *S-conical Gauss map and dual s-conical minimal surface.* The vertices of the circumscribed Koebe polyhedron that corresponds to the circle pattern can now be easily found by inverting the euclidean centers of the circles at the  $S^2$  (the cone tips are the polar points to the planes containing the circles). These vertices furnish an s-conical Gauss map. Its Koenigs-dual therefore is an s-conical minimal surface.

## 7 Classical surfaces

### 7.1 Schwarz H and Schoen I6 surfaces

The Schwarz H surface, see Figure 5 (left), is a triply periodic minimal surface which was already known to H. A. Schwarz, see [Sch90, vol. 1, pp. 92–125]. To understand the boundary conditions take the edges of two parallel copies of an equilateral triangle as boundary frame for a minimal surface spanned in between them. Then there is one plane of reflectional symmetry parallel to the triangles and three other orthogonal planes forming the symmetry group of the equilateral triangle. Thus a fundamental piece is bounded by three planar curvature lines and one straight asymptotic line, see Figure 5,

bottom. Its image under the Gauss map is a spherical triangle with angles  $\frac{\pi}{2}, \frac{\pi}{2}, \frac{\pi}{3}$ . The two parameters  $n, m$  of the curvature line combinatorics correspond to the side length of the equilateral triangle and to their distance.

Analogous to the construction of the Schwarz H surface we construct Schoen's I6 surface. The only difference is the boundary angles of the fundamental piece in the Gauss image. Here we have  $\frac{\pi}{4}$  instead of  $\frac{\pi}{3}$  at the respective corner.

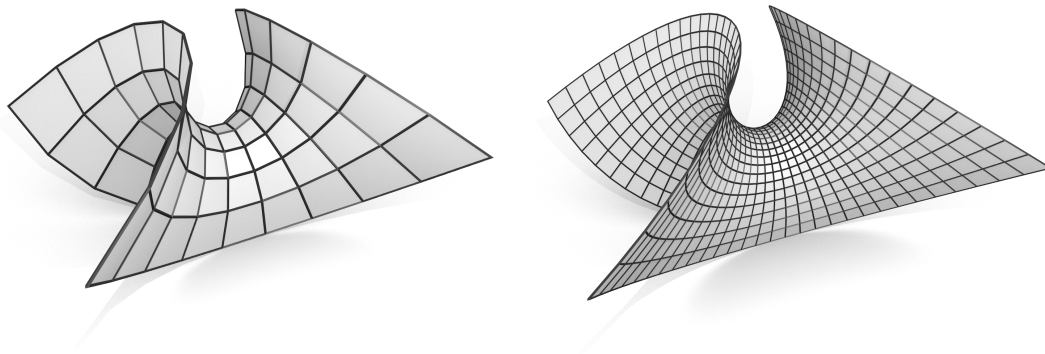


Figure 6: S-conical Enneper surface, two resolutions.

## 7.2 Enneper

The circle pattern on the sphere belonging to Enneper's surface can be obtained by stereographic projection of a regular square grid. The s-conical Gauss map of Enneper's surface is the dual grid of this pattern where a vertex is the pole of the respective plane of the circle. The surface is obtained by dualization of the quadrilaterals, see Figure 6.

## 7.3 Schwarz P

The curvature line pattern of a fundamental piece of the Schwarz P surface has regular square grid combinatorics and is bounded by four planar curvature lines, see Figure 7. The intersection angles at the corners of the fundamental piece are right angles for three of the corners and  $\frac{\pi}{6}$  at the fourth corner. We create the fundamental piece directly on the sphere using the spherical functional with prescribed boundary angles.

In the Gauss image the fundamental piece covers exactly  $\frac{1}{24}$  of the sphere and can be mirrored to obtain the whole sphere. This suggests an alternative construction of the Schwarz P surface by means of a full symmetric spherical circle patterns with the combinatorics of the cube using the euclidean functional. We invoke stereographic projection and Möbius normalization. The circle pattern is symmetric if the center of mass of the circle intersections is the center of the sphere. There is always a Möbius transformation of the sphere such that moves the center of mass to the center of the sphere [Spr05].



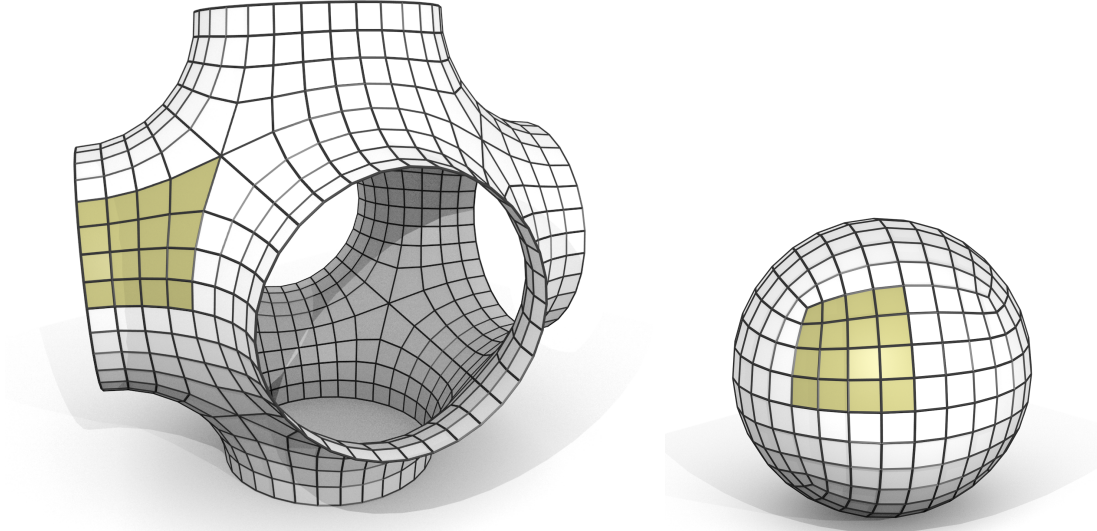


Figure 7: S-conical Schwarz P surface with fundamental piece (hi-lighted). S-conical Gauss map with fundamental piece (right). The sphere is doubly covered to create the surface.



Figure 8: S-isothermic Scherk tower and its Gauss map (left and middle). Associate discrete minimal surface with  $\psi = \pi/2$  (right).

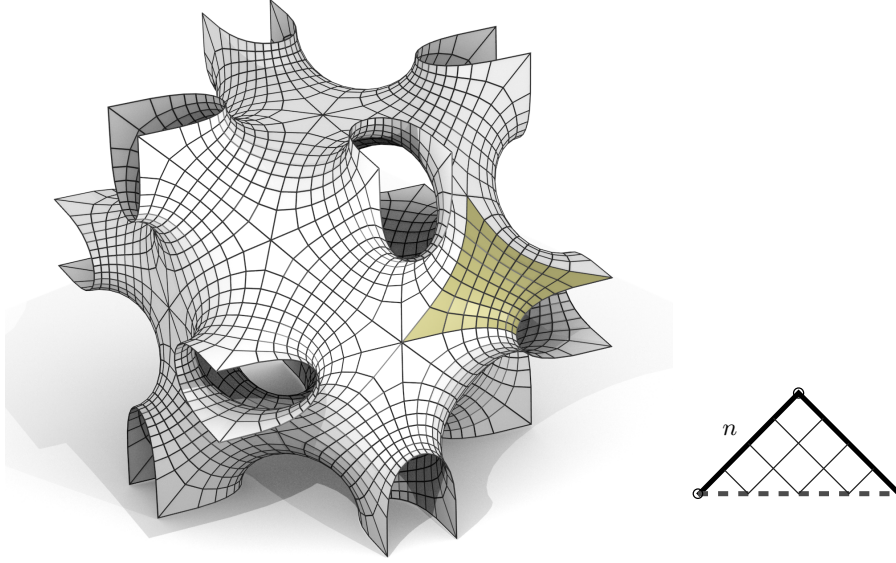


Figure 9: S-conical Neovius's surface (left). Combinatorial curvature line parametrization of a fundamental piece (right). For the construction of the surface we use a bigger fundamental piece bounded by planar curvature lines only (hi-lighted).

#### 7.4 Scherk Tower

Scherk's saddle tower is a simply periodic minimal surface, that is asymptotic to two intersecting planes, see, e.g., [Kar89]. There is a 1-parameter family, the parameter corresponding to the angle between the asymptotic planes, see Figure 8 (left). When mapped to the sphere by the Gauss map, the curvature lines of the Scherk tower form a pattern with four special points, which correspond to the four half-planar ends. A loop around a special point corresponds to a period of the surface. In a neighborhood of each special point, the pattern of curvature lines behaves like the image of the standard coordinate net under the map  $z \mapsto z^2$  around  $z = 0$ . In the discrete setting, the special points are modeled by pairs of 3-valent vertices, see Figure 8 (middle). The combinatorics of the circle pattern that we use to construct the Gauss map is the dual of the discrete Gauss map. Thus every 3-valent vertex corresponds to a circle in the pattern. The ratio  $m : n$  corresponds to the parameter of the smooth case. By Koebe's theorem, there exists a corresponding circle pattern, which is made unique by Möbius normalization such that the center of mass is the center of the sphere.

#### 7.5 Neovius's Surface

H. A. Schwarz [Sch90] began to consider minimal surfaces bounded by two straight lines and an orthogonal plane. His student E. R. Neovius continued and deepened this study and found another triply periodic surface, see [Neo83]. This surface has the same

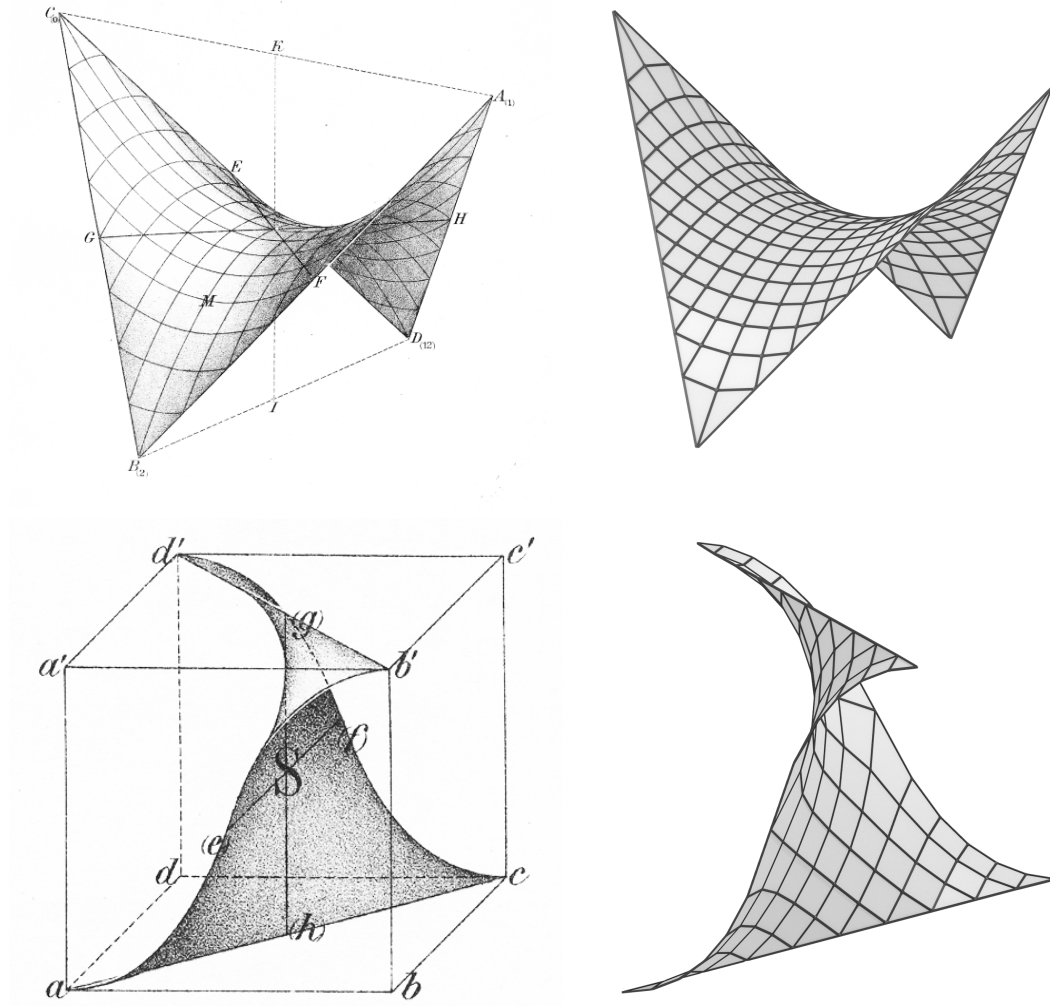


Figure 10: Comparison of discrete minimal surfaces to classical images. Quadrilateral boundary surface and corresponding s-conical minimal surface (top). Gergonne's surface and s-conical minimal surface (bottom). Drawings by H. A. Schwarz [Sch90].

symmetry group as Schwarz P surface and was named  $C(P)$  by A. Schoen, see Figure 9 (left).

The fundamental piece of Neovius's surface that we use for construction is bounded by four planar curvature lines. Its Gauss image forms a spherical quadrilateral with angles  $\frac{3\pi}{4}, \frac{2\pi}{6}, \frac{\pi}{2}, \frac{2\pi}{6}$ . Such a fundamental piece is symmetric with respect to a  $180^\circ$ -rotation. One could also consider this reduced piece to create the surface, see Figure 9 (right). The discrete parameter corresponds to the resolution of discretization.

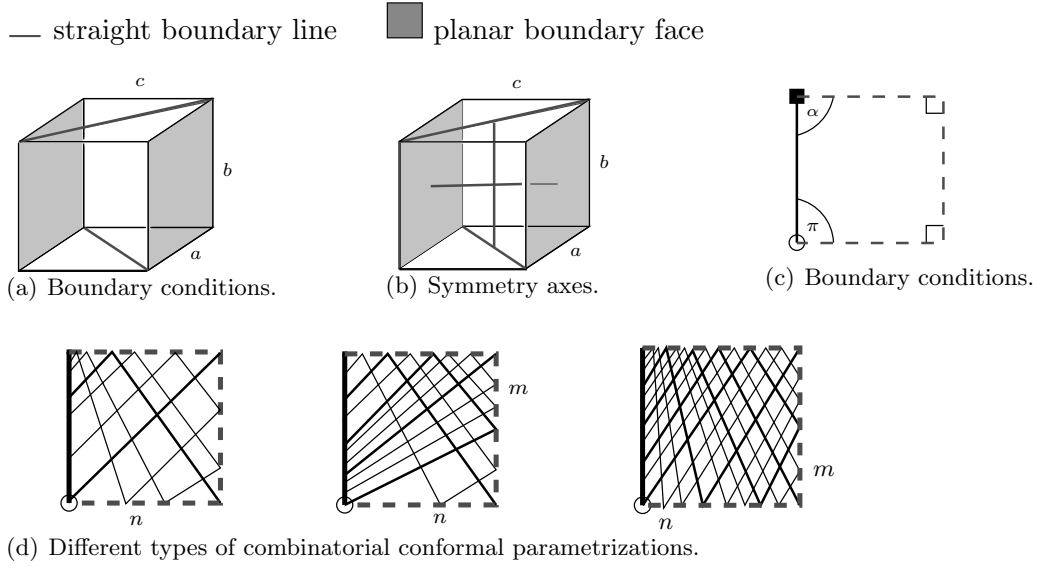


Figure 11: Gergonne's surface: boundary conditions and combinatorial conformal parametrizations.

## 7.6 Gergonne's surface

Gergonne's surface, see Figure 10 (bottom), traces back to J. D. Gergonne [Ger16], who posed the first geometric problem leading to minimal surfaces with free boundaries in 1816. A correct solution was only found by H. A. Schwarz in 1872; see [Sch90, pp. 126–148].

Given a cuboid take two opposite faces as boundary faces and non-collinear diagonals of two other opposite faces, as in Figure 11(a). Then the two axes of  $180^\circ$ -rotational symmetry, see Figure 11(b), will lie on the minimal surface and cut it into four congruent fundamental pieces bounded by three straight asymptotic lines and one planar curvature line, see Figure 11(c). Its images under the Gauss map are spherical triangles with angles  $\frac{\pi}{2}$ ,  $\frac{\pi}{2}$ , and  $\alpha$ .

A combinatorial picture of the curvature lines is shown in Figure 11(d). The two parameters correspond to the free choice of two length parameters of the cuboid, given the angle  $(\frac{\pi}{2} - \alpha)$  between the diagonal and the planar boundary face. If  $\alpha = \frac{\pi}{4}$ , the minimal surface can be continued by reflection and rotation in the boundary faces/edges to result in a triply periodic (discrete) minimal surface.

## 7.7 Catenoid and helicoid

For the s-conical helicoid we can explicitly construct the corresponding circle pattern. It is the S-Exp pattern [BP99], a discretization of the exponential map. The underlying quad-graph is  $\mathbb{Z}^2$ , with circles corresponding to points  $(m, n)$  with  $m + n \equiv 0 \pmod{2}$ .

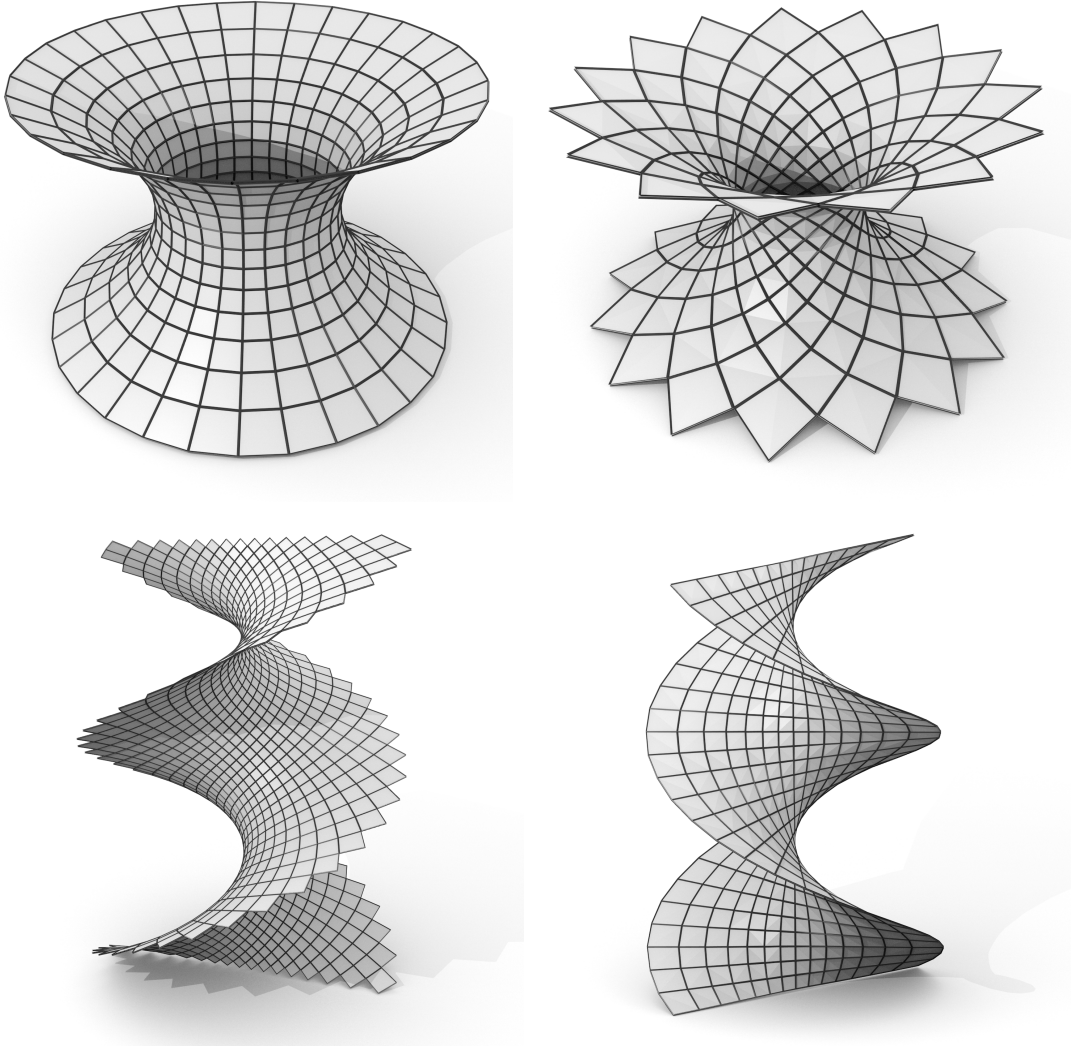


Figure 12: Discrete  $s$ -conical catenoid (top) and helicoid (bottom). Asymptotic line parametrizations in the associated family (right).

The centers  $c(n, m)$  and the radii  $r(n, m)$  of the circles are

$$c(n, m) = e^{\alpha n + i\rho m}, \quad r(n, m) = \sin(\rho) |c(n, m)|,$$

where

$$\rho = \pi/N, \quad \alpha = \operatorname{arctanh}\left(\frac{1}{2} |1 - e^{2i\rho}|\right).$$

The corresponding S-conical minimal surface is shown in Figure 12 (bottom left). In the associated family at  $\psi = \frac{\pi}{2}$  of the discrete helicoid we have the discrete catenoid parametrized along asymptotic lines. It is shown in Figure 12 (top right).

## 8 The Associated Family

Classical minimal surfaces come in one-parameter families whose members are isometric to each other and share the same Gauss map. Geometrically, the partial derivative vectors of the parametrized surface get rotated around the normal direction by a constant angle — the one parameter of the family. The previous discretizations of isothermally parametrized minimal surfaces come with this kind of family as well — rotation of partial derivatives gets replaced by appropriate rotations of edges. This has been discussed in [BHS06] and [HSFW14].

Here we present a similar process for our s-conical minimal surfaces: by, with slight adjustments, rotating edges around edge normals we find a family of discrete surfaces. We then show that all naturally occurring normal directions as well as a notion of metric coefficients are preserved within this family.

In this section, let  $n$  always be an s-conical Gauss map with circle pattern angle  $\sigma$  and  $f$  its dual s-conical minimal surface. We always assume the scaling of  $f$  is such that the lengths of its diagonal segments — which are just the radii of the spheres centered at the vertices — are the inverse of the length of the respective segments in  $n$ .

**Theorem and Definition 12.** Let  $n$  be an s-conical Gauss map and  $f$  its dual s-conical minimal surface on a simply connected quad-graph. Let  $e = f_i - f$  be an edge of  $f$ ,  $g = n_i - n$  the corresponding edge of  $n$ , and  $N$  the face normal of an adjacent face. Let  $\psi$  be any angle. Then we can define

- i) an *edge normal*  $E$  as the direction given by the closest point to the origin on  $g$ ;
- ii) the angle  $\alpha$  formed by  $E$  and  $N$  (also cf. figure 14);
- iii) a scaling factor

$$\lambda := \sqrt{1 + \sin^2 \psi \tan^2 \alpha};$$

- iv) a rotation angle  $\varphi$  satisfying

$$\cos \varphi = \frac{1}{\lambda} \cos \psi, \quad \sin \varphi = \frac{1}{\lambda} \frac{\sin \psi}{\cos \alpha};$$

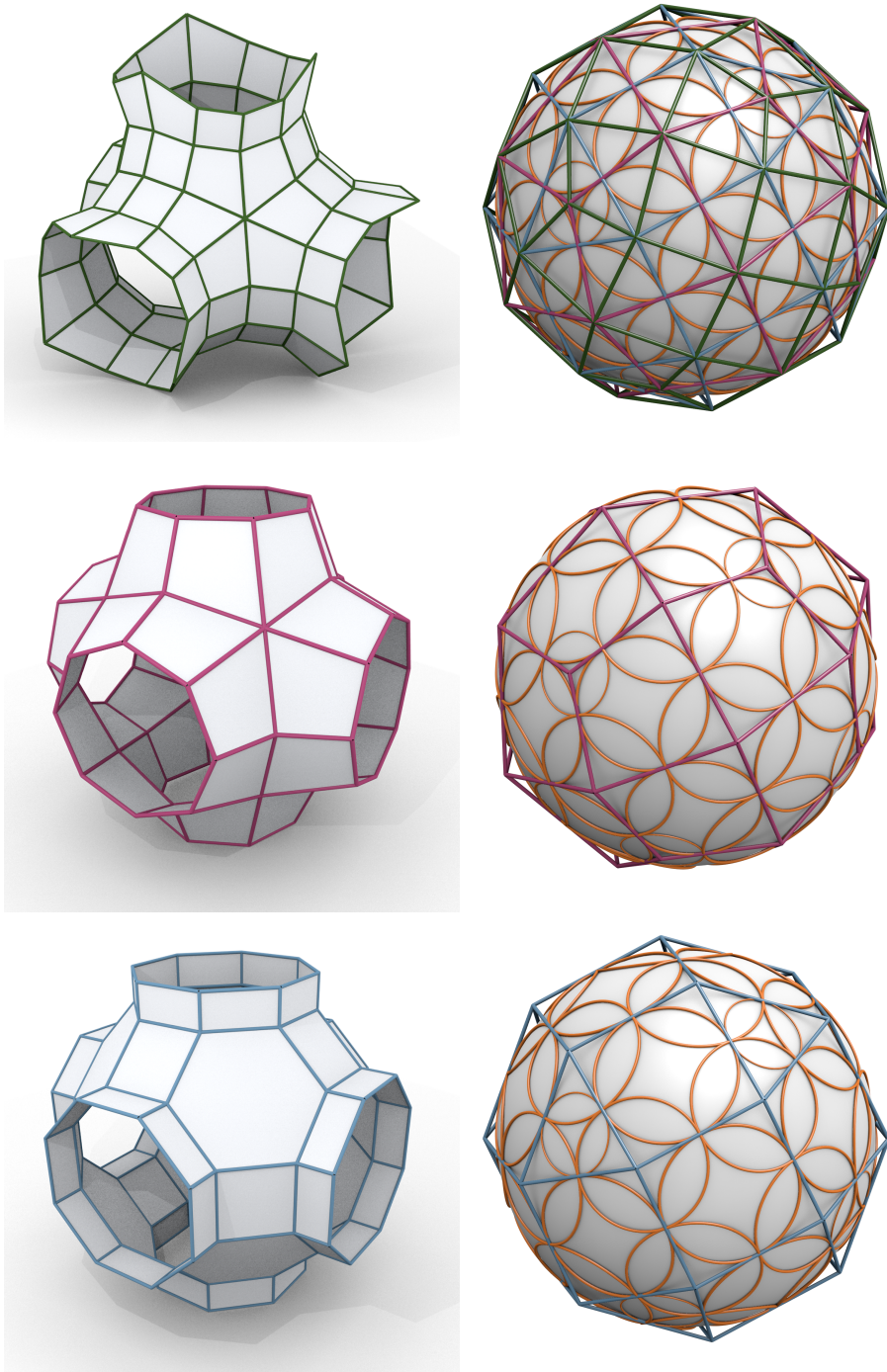


Figure 13: Discrete minimal surfaces and corresponding discrete Gauss maps.  $S$ -conical minimal surface and  $s$ -conical Gauss map (top).  $S$ -isothermic surfaces (middle and bottom).



v) and a transformed edge  $e^\psi$  by rotating  $\lambda e$  around  $E$  by  $\varphi$ .

Neither of these quantities depend on the choice of adjacent face. For each quadrilateral of  $f$ , its four transformed edges again close to a (in general non-planar) quadrilateral, and we get a transformed surface  $f^\psi$ . The family of these  $f^\psi$  is called the *associated family* of  $f$ .

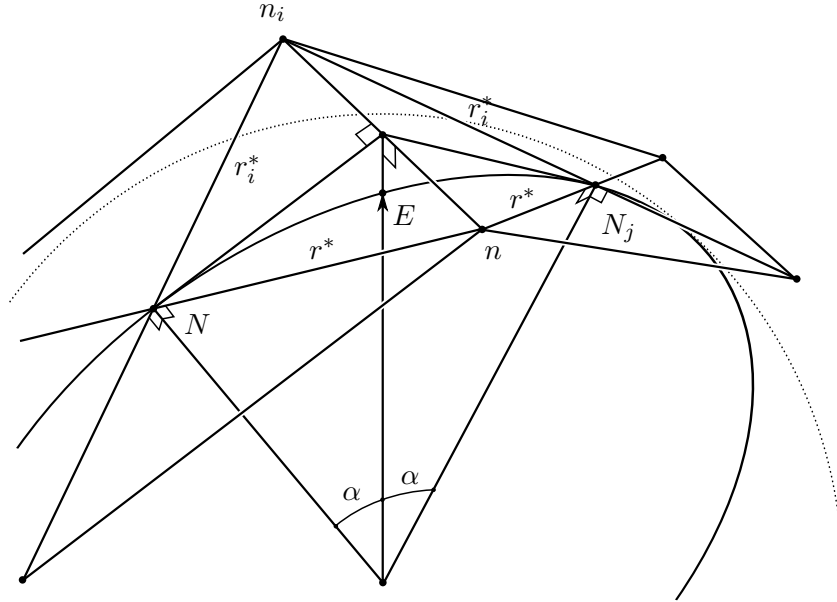


Figure 14: The edge normal

We collect the calculation steps needed for the proof in several lemmata.

**Lemma 13.** *None of the quantities  $E$ ,  $\alpha$ ,  $\lambda$ ,  $\varphi$  and  $e^\psi$  defined above depend on the choice of the face adjacent to  $g$ .*

*Proof.* The only definition directly involving this choice is the one of  $\alpha$ , so this is the one we have to check. But the normals  $N$ ,  $N_i$  of the adjacent faces are both the tangent points of planes containing  $g$  to the unit sphere. Therefore the situation is completely symmetric with respect to the plane containing  $g$  and the origin. In particular,  $E$  is the angle bisector of  $N$  and  $N_j$ , and  $\alpha$  is just half the angle between the face normals.  $\square$

Now we look at the individual quadrilaterals.

**Lemma 14.** *Let  $P$  denote the plane of the adjacent face with normal  $N$ . Then the projection  $e_P^\psi$  of  $e^\psi$  into  $P$  is just  $e$  rotated around  $N$  by  $\psi$ .*

*Proof.* As depicted in figure 15, consider the spherical triangle formed by the normalizations of  $e$ ,  $e^\psi$  and  $e_P^\psi$ . It has a right angle at  $e_P^\psi$ , and the angle at  $e$  is  $\alpha$ . The length



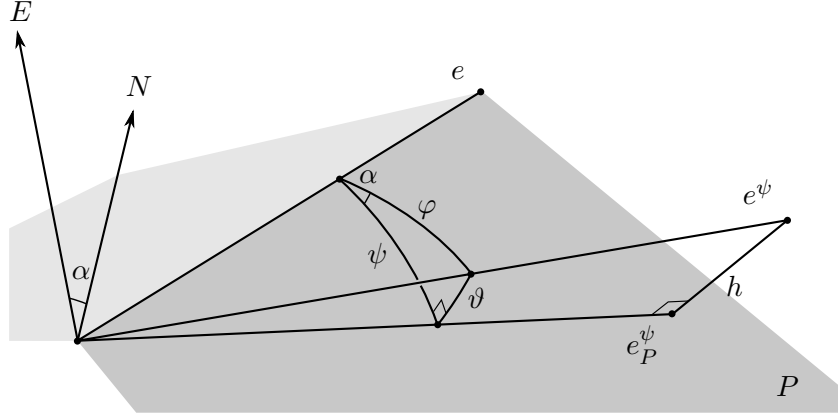


Figure 15: The rotated and rescaled edge and its projection into  $P$

of its hypotenuse  $ee^\psi$  is  $\varphi$ . Denote the angle formed by  $e^\psi$  and  $e_P^\psi$ , i.e. the length of the edge  $e^\psi e_P^\psi$  in the triangle, by  $\vartheta$ . Identities from spherical trigonometry yield

$$\tan \vartheta = \sin \psi \tan \alpha$$

and therefore

$$\cos \vartheta = \frac{1}{\lambda};$$

they further confirm that our choice of  $\varphi$  is the right one for the side  $ee_P^\psi$  to have length  $\psi$ .

Since the length of the projection satisfies  $|e_P^\psi| = \cos \vartheta |e^\psi|$ , our rescaling factor  $\lambda$  precisely conserves projected length.  $\square$

As we want the actual transformed edges  $e^\psi$  to form closed quadrilaterals, we still have to consider the — with respect to face planes — vertical component. We begin with its absolute value in order to avoid working with signed angles. First, we note that we know something about the lengths of the original edges:

**Lemma 15.** *The length of  $e$  is*

$$|e| = \cot \alpha \sin \sigma,$$

where  $\sigma$  is the (globally constant) circle pattern angle.

*Proof.* First consider the triangle  $(n, n_i, N)$  formed by the corresponding edge  $g$  and adjacent diagonal segments of the corresponding face in the Gauss map. The lengths of its diagonal segment are  $r^*$  and  $r_i^*$ . Its angle at  $N$  is  $\sigma$  (or  $\pi - \sigma$ , which would give the same result). The height connecting  $N$  and the edge  $g$  in this triangle is

$$\sin \sigma \frac{r^* r_i^*}{|g|} = \tan \alpha$$

since the point on  $g$  closest to  $N$  is just the edge normal  $E$ : both  $N$  and  $E$  lie in the plane orthogonal to  $g$  through the origin. So

$$\frac{|g|}{r^* r_i^*} = \cot \alpha \sin \sigma.$$

In our choice of scaling, this was precisely the length  $|e|$  of the dual edge.  $\square$

**Lemma 16.** *The absolute height of  $e^\psi$  in  $N$ -direction is*

$$h = \sin \psi \sin \sigma.$$

*Proof.* As above, let  $\vartheta$  be the angle formed by  $e^\psi$  and the face plane. By spherical trigonometry,

$$\sin \vartheta = \sin \varphi \sin \alpha,$$

and recalling the definition of  $\varphi$  and using lemma 15 we calculate

$$h = \sin \vartheta |e^\psi| = \sin \psi \sin \sigma.$$

$\square$

**Lemma 17.** *The sign of the  $N$ -component of  $e^\psi$  alternates around each face.*

*Proof.* For each edge of a quadrilateral, let  $p$  be the the point on  $g$  closest to the origin (such that  $E = \frac{p}{\|p\|}$ ). Since  $p - N$ ,  $g$  and  $N$  are orthogonal, we can identify our  $\mathbb{R}^3$  with  $\text{Im } \mathbb{H}$  by orientation-preserving isometry such that

$$p - N = d\mathbf{i}, \quad e = l\mathbf{j}, \quad N = \mathbf{k} \text{ for some } d > 0, l \in \mathbb{R}.$$

Then, always up to positive factor,  $E \sim d\mathbf{i} + \mathbf{k}$ , and our transformed edge is

$$e^\psi \sim \left( s \cos \left( \frac{\varphi}{2} \right) + \sin \left( \frac{\varphi}{2} \right) (d\mathbf{i} + \mathbf{k}) \right) l\mathbf{j} \left( \left( s \cos \left( \frac{\varphi}{2} \right) - \sin \left( \frac{\varphi}{2} \right) (d\mathbf{i} + \mathbf{k}) \right) \right).$$

with some further positive factor  $s > 0$ . We calculate its  $\mathbf{k}$ -component and find it to be positively proportional to

$$l \cos \left( \frac{\varphi}{2} \right) \sin \left( \frac{\varphi}{2} \right).$$

From the definition of  $\varphi$  we see that  $\varphi$  is in the same quadrant as  $\psi$ , independently of  $\alpha \in [0, \frac{\pi}{2}]$ . So the signs of  $\cos \left( \frac{\varphi}{2} \right)$  and  $\sin \left( \frac{\varphi}{2} \right)$  are the same for each edge of our quadrilateral.

Therefore our desired sign is just given by the orientation of  $(p - N, e, N)$ ; since  $N$  is the same for all edges, by the orientation of  $(p - N, e)$  within the face plane  $P$ . Let  $v_1, v_2$  be the normalized diagonal directions; our quadrilateral is then  $(a_1 v_1, a_2 v_2, a_3 v_1, a_4 v_2)$  for some  $a_1, \dots, a_4 \in \mathbb{R} \setminus \{0\}$  (with the diagonal intersection point  $N$  as the origin of  $P$ ). The (non-rotated) dual quadrilateral is, up to global scaling,  $(-\frac{1}{a_1} v_2, -\frac{1}{a_2} v_1, -\frac{1}{a_3} v_2, -\frac{1}{a_4} v_1)$ .

Now for each edge  $g = a_n v_j - a_m v_i$  (with  $i \neq j \in \{1, 2\}$ ), we find  $p$  to be given (within  $P$ ) as

$$p = \frac{a_m a_n}{a_m^2 + a_n^2 - 2a_m a_n \langle v_i, v_j \rangle} ((a_m - a_n \langle v_i, v_j \rangle) v_j + (a_n - a_m \langle v_i, v_j \rangle) v_i).$$

We calculate the desired orientation of  $(p - N, e)$  (within  $P$ ):

$$\begin{aligned} \det(p, e) &= \frac{a_m a_n}{a_m^2 + a_n^2 - 2a_m a_n \langle v_i, v_j \rangle} \\ &\quad \cdot \det \left( (a_m - a_n \langle v_i, v_j \rangle) v_j + (a_n - a_m \langle v_i, v_j \rangle) v_i, \frac{1}{a_m} v_j - \frac{1}{a_n} v_i \right) \\ &= \frac{a_m a_n}{a_m^2 + a_n^2 - 2a_m a_n \langle v_i, v_j \rangle} \left( \frac{a_m - a_n \langle v_i, v_j \rangle}{a_n} + \frac{a_n - a_m \langle v_i, v_j \rangle}{a_m} \right) \det(v_i, v_j) \\ &= \det(v_i, v_j). \end{aligned}$$

Since  $(i, j)$  alternates between being  $(1, 2)$  and  $(2, 1)$  around our quadrilateral, the orientation indeed alternates, and so does the sign of  $\langle e^\psi, N \rangle$ .  $\square$

*Proof of the claims in theorem and definition 12.* By the lemmata 14 through 17, we see that for each quadrilateral, the transformed edges close to form a new (not necessarily planar) quadrilateral. By lemma 13, the edges of adjacent transformed quadrilaterals fit together just by translation, so they patch together around each vertex. By simple connectedness of the domain, they form a well-defined surface.  $\square$

We collect some important properties of  $f^\psi$  we have seen in the construction in

**Corollary 18.** *i) For each face of  $f$ , with  $P$  its plane, the projection of the corresponding face of  $f^\psi$  into  $P$  is (up to translation) just the original face rotated by  $\psi$  around the face normal  $N$ .*

*ii) The diagonals of each face of  $f^\psi$  are parallel to their corresponding diagonal in  $f$  rotated around  $N$  by  $\psi$  and retain their length.*

*iii) The diagonals of each face of  $f^\psi$  have distance  $h = \sin \psi \sin \sigma$  to each other.*

In the classical theory of minimal surfaces, the metric and the Gauss map is preserved in the associated family. In the s-conical case, we can look at the spheres centered at the vertices and meeting in the diagonal intersection points and interpret their radii  $r$  as a metric parameter: a coefficient at each vertex such that lengths of diagonals are the sum of the values at the adjacent vertices. Surface normals come in three variants: vertex normals are the cone axes, their direction given by the vertices of the Gauss map  $n$ ; face normals are obvious for the planar faces, and here their direction coincides with the diagonal intersection points of the Gauss map; edge normals  $E$  have been defined in theorem and definition 12 above.

From what we have seen, it is most natural to make the following definitions, giving names to the different types of normals and the metric coefficient in the associated family:

**Definition 13.** Let  $f^\psi$  be in the associated family of an s-conical minimal surface.

- i) The *face normals*  $N^\psi$  are the directions orthogonal to both diagonals of the face. We choose their orientation w.r.t. directed diagonals to be the same as that of  $N$  w.r.t. the correspondingly directed diagonals of  $f$ .
- ii) The angle bisector of two adjacent face normals is orthogonal to the common edge; we define it to be the *edge normal*  $E^\psi$ .
- iii) For each face adjacent to a fixed vertex of  $f^\psi$ , consider the triangle formed by the edges containing the vertex. These triangles are tangent to a common cone with tip at the vertex; we define its axis to be the *vertex normal* direction  $n^\psi$ . Its orientation is again set to be the same as that of  $n$  w.r.t. the corresponding edges of  $f$ .
- iv) On the two diagonals of each face we denote the points closest to the respective other diagonal by  $o^\psi$  and  $\tilde{o}^\psi$  (at the moment, in our notation we do not care for the attribution to the specific diagonals). By the definition of  $N^\psi$  above,  $o^\psi - \tilde{o}^\psi \parallel N^\psi$ . Cf. figure 16.
- v) On each outgoing diagonal of a fixed vertex of  $f^\psi$ , consider the point  $o^\psi$  (or  $\tilde{o}^\psi$ ). These points lie on a sphere centered at the vertex; we define its radius to be the *metric coefficient*  $r^\psi$  at the vertex.

The existence of the spheres allowing for the definition of the metric coefficients will be shown together with

**Theorem 19.** *The vertex, edge and face normals as well as the metric coefficients are preserved in the associated family:*

*Let  $f$  be an s-conical minimal surface with  $n$  its dual s-conical Gauss map and  $f^\psi$  be in the associated family  $f$ .*

- i)  $N^\psi = N$ , where  $N$  is the face normal map of  $f$  and  $n$ .
- ii)  $E^\psi = E$ , where  $E$  is the edge normal map of  $f$  and  $n$  as defined in theorem and definition 12.
- iii)  $n^\psi = n$
- iv)  $r^\psi = r$ , where  $r$  are the sphere radii of  $f$ .

*Proof.* i) Follows directly from 18, part ii).

- ii) By definition, the edges of  $f^\psi$  are orthogonal to  $E$ , and by i) the angle bisector of adjacent  $N^\psi$  is still  $E$ .
- iii) Will follow from the next proposition and its corollary 21.

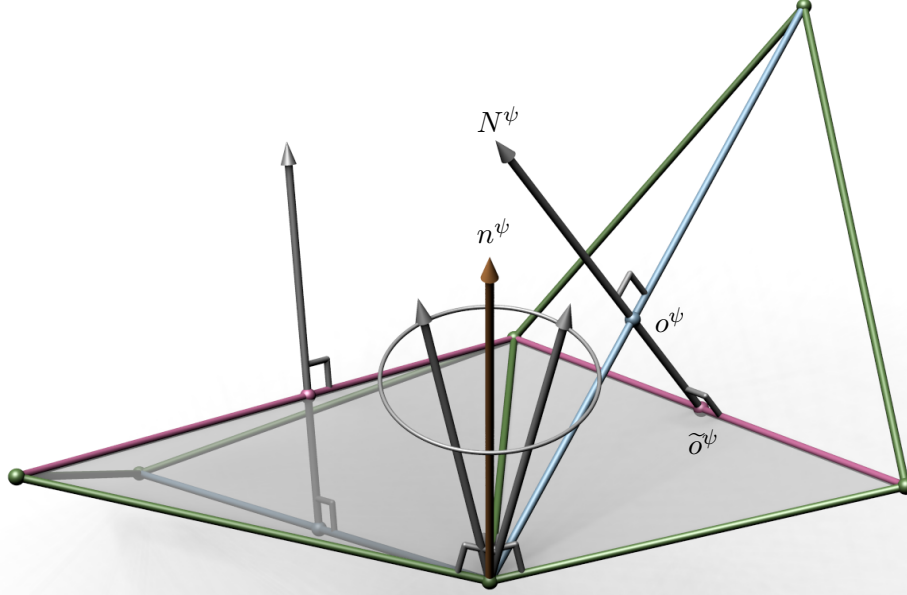


Figure 16: A vertex normal and two face normals in the associated family. The normals of the triangles adjacent to the front center vertex lie on a circle around the vertex normal. The face normals are orthogonal to both diagonals.

- iv) By 18, part ii), up to rotation around  $N$ , the diagonals projected into the plane  $P$  orthogonal to  $N$  are just the original diagonals of  $f$ . Since  $N$  is orthogonal to both diagonals of  $f^\psi$ , in the projection their closest points become the intersection point. So the distances from vertices to the closest points are the same as the distances of vertices and diagonal intersection points of  $f$ , where we knew the spheres existed.

□

**Proposition 20.** *Let  $n$  be an  $s$ -conical Gauss map and  $f$  its dual  $s$ -conical minimal surface. Then for each vertex  $f^\psi$  and adjacent face of  $f^\psi$ , the angle  $\nu$  between the vertex normal  $n$  and the normal  $\tilde{N}$  of the plane spanned by the vertex and its two neighboring ones in the face satisfies*

$$\cos \nu = \sqrt{\cos^2 \kappa + \sin^2 \kappa \sin^2 \psi},$$

where  $\kappa$  is the angle formed by  $n$  and the original face normal  $N$ .

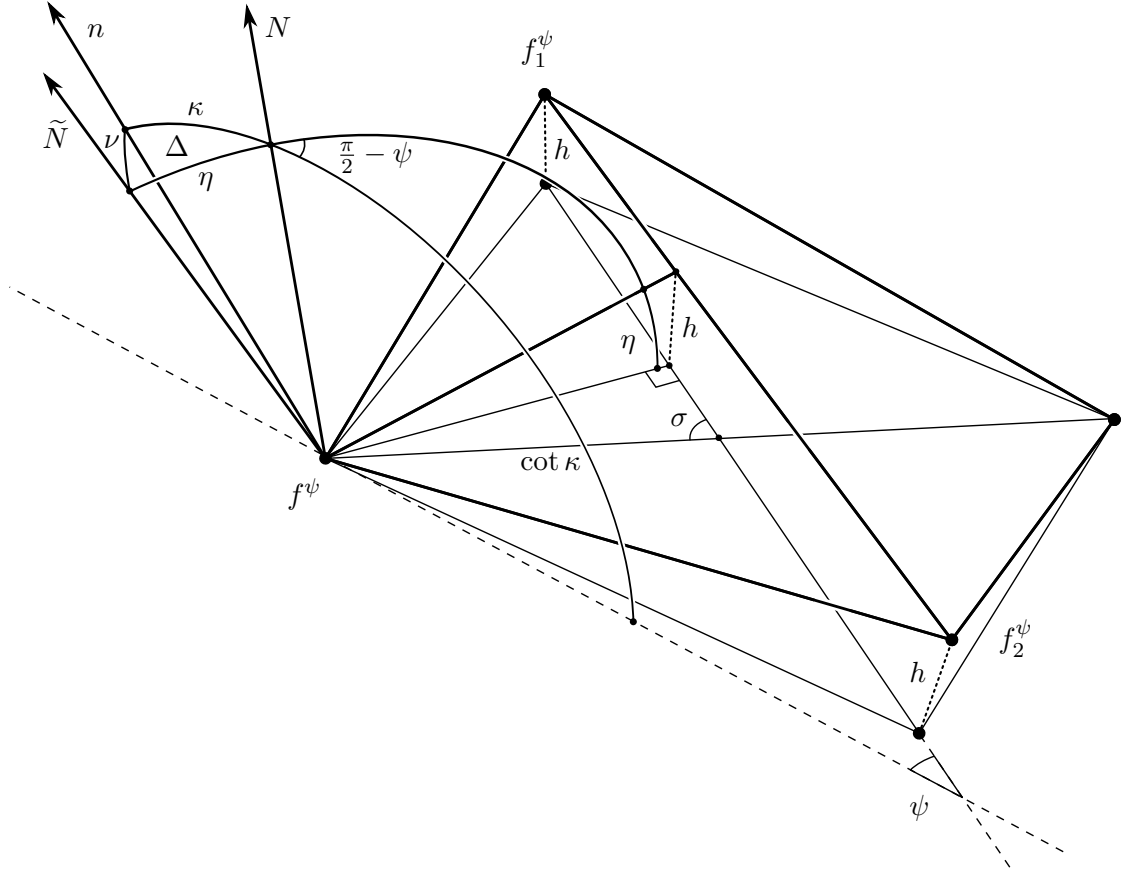


Figure 17: The configuration in proposition 20

*Proof.* For an overview of the situation, we provide figure 17. We look at the spherical triangle  $\Delta$  formed by  $N$ ,  $n$  and  $\tilde{N}$  with sides  $\kappa$ , the angle  $\eta$  formed by  $N$  and  $\tilde{N}$  and the desired  $\nu$ . We can calculate  $\nu$  from  $\eta$  and the angle at  $N$ .

Note that w.l.o.g. we consider, as depicted in figure 17, the case where  $f_{\pm 1}^\psi$  and  $f_{\pm 2}^\psi$  lie above  $f^\psi$  with respect to  $N$ . In the other case, both sides  $\kappa$  and  $\eta$  of  $\Delta$  change orientation, leaving the angle at  $N$  unchanged.

Let  $Q$  be the original (planar) quadrilateral of  $f$  and  $P$  the plane parallel to  $Q$  sitting at our vertex  $f^\psi$ ; by  $Q^\psi = (f^\psi, f_1^\psi, f_{12}^\psi, f_2^\psi)$  we denote the (non-planar) quadrilateral of  $f^\psi$  (Since we are looking at just one fixed quadrilateral, we use this notation regardless of any actual grid directions, in particular, the same notation applies for a vertex with valency other than 4). By corollary 18, i), the projection  $Q_P^\psi$  of  $Q^\psi$  into  $P$  is  $Q$  rotated around  $N$  by  $\psi$ .

By definition of s-conical Gauss maps, the projection of the cone axis  $n$  into  $P$ , indicated in figure 17 by a dashed line, is parallel to the diagonal  $nn_{12}$ , so by duality it is parallel to the diagonal  $f_1f_2$  of  $Q$  and consequently forms the angle  $\psi$  with the diagonal of  $Q_P^\psi$  not containing the vertex  $f^\psi$ . Since the plane through  $f^\psi$  spanned by

the directions  $N$  and  $\tilde{N}$  is perpendicular to this diagonal, the angle at  $N$  in  $\Delta$  is  $\frac{\pi}{2} - \psi$ .

The side  $\eta$  in this triangle is the angle between  $P$  and the triangle  $f^\psi$ ,  $f_1^\psi$  and  $f_2^\psi$ ; we can calculate it as follows: The length of the diagonal segment at  $f^\psi$  of  $Q_P^\psi$  is  $\cot \kappa$ , since the corresponding length in the Gauss map is  $\tan \kappa$ . The distance from  $f^\psi$  to the other diagonal of  $Q_P^\psi$  is therefore  $\sin \sigma \cot \kappa$ , so

$$h = \sin \sigma \cot \kappa \tan \eta;$$

but by lemma 16 we also know

$$h = \sin \psi \sin \sigma.$$

So we know

$$\tan \eta = \sin \psi \tan \kappa.$$

Now we can use trigonometric identities to calculate

$$\begin{aligned} \cos \nu &= \cos \kappa \cos \eta + \sin \kappa \sin \eta \cos \left( \frac{\pi}{2} - \psi \right) \\ &= \cos \kappa \cos(\arctan(\sin \psi \tan \kappa)) + \sin \kappa \sin(\arctan(\sin \psi \tan \kappa)) \sin \psi \\ &= \sqrt{\cos^2 \kappa + \sin^2 \kappa \sin^2 \psi}. \end{aligned}$$

□

The preceding result allows us to notice that, in a non-planar sense, the conicality property survives in the associated family:

**Corollary 21.** *For each vertex  $f^\psi$  of the transformed surface, the adjacent half-face triangles are still tangent to a common cone with tip at the vertex and axis direction  $n$ .*

*Proof.* Since  $f$  was conical,  $\kappa$  was constant around each vertex. Therefore  $\nu$  is constant as well. □

For classical minimal surfaces, the member of the associated family rotated out of curvature line parametrization by  $\psi = \frac{\pi}{2}$ , called the *conjugate* minimal surface, is parametrized asymptotically. Recalling that a discretization of asymptotically parametrized surfaces is given by nets with planar vertex stars — called A-nets, see e.g. [BS08] —, we see that our discretization shares this property:

**Corollary 22.** *For  $\psi = \frac{\pi}{2}$ , the transformed surface  $f^\psi$  is a discrete asymptotic net.*

*Proof.* Proposition 20 yields  $\cos \nu = 1$ , and this precisely means planar vertex stars. □

For use later on, we note that from the proof of proposition 20 we can calculate the distance of diagonals and vertices (of the same face): for each vertex of  $f^\psi$ , the diagonals not originating at the vertex of all adjacent faces have distance

$$d = \sqrt{h^2 + \cot^2 \kappa \sin^2 \sigma} = \sqrt{\sin^2 \psi \sin^2 \sigma + \cot^2 \kappa \sin^2 \sigma} = \sin \sigma \sqrt{\cot^2 \kappa + \sin^2 \psi} \quad (6)$$

to the vertex.

Another fact we note for later use is

**Corollary 23.** For  $\psi = \frac{\pi}{2}$ , the point on a diagonal closest to both vertices not contained in the diagonal is  $o^\psi$  (or  $\tilde{o}^\psi$ , whichever lies on that particular diagonal).

*Proof.* In this case, the other diagonal and the line through  $o^\psi$  and  $\tilde{o}^\psi$  with direction  $N$  span the plane perpendicular to the diagonal being considered, so in particular, the vertices in question as well as  $o^\psi$  and  $\tilde{o}^\psi$  are contained in that plane.  $\square$

## 9 A Weierstrass Representation

The classical Weierstrass representation allows to compute minimal surfaces from holomorphic data (generally on the underlying Riemann surface). In [BHS06] a discrete version of the Weierstrass representation was given for s-isothermic minimal surfaces. There, starting from a circle pattern, a discrete s-isothermic minimal surface and its associated family can be computed directly, fusing the steps of getting the Gauss map from the pattern and then dualizing into one formula. The same can be done for s-conical minimal surfaces:

**Theorem 24.** Let  $c : V(D) \rightarrow \mathbb{C}$  be the circle centers of an constant angle circle pattern. For a pair of neighboring circles with centers  $c_1$  and  $c_2$  let  $p$  denote the point of intersection to the right of the edge from  $c_1$  to  $c_2$ . Then the vertices of the corresponding conical minimal surface at parameter  $\psi$  in the associated family satisfy

$$f(c_2) - f(c_1) = \pm \operatorname{Re} \left[ \left( \frac{2}{1 + |p|^2} \left( R(c_1) \frac{\bar{c}_2 - \bar{p}}{|c_2 - p|} - R(c_2) \frac{\bar{c}_1 - \bar{p}}{|c_1 - p|} \right) \begin{pmatrix} 1 - p^2 \\ i(1 + p^2) \\ 2p \end{pmatrix} \right) - i \frac{d_p s(c_1 - p)}{\|d_p s(c_1 - p)\|} \times \frac{d_p s(c_2 - p)}{\|d_p s(c_2 - p)\|} \right] e^{i\psi} \quad (7)$$

$$R(c_i) = \frac{1 + |c_i|^2 - |c_i - p|^2}{2|c_i - p|} \quad (8)$$

where the sign depends on a chosen edge labeling of (the edge-bipartite)  $D$  and

$$d_p s(z) = \operatorname{Re} \left[ \frac{2\bar{z}}{1 + |p|^2} \begin{pmatrix} 1 - p^2 \\ i(1 + p^2) \\ 2p \end{pmatrix} \right].$$

*Proof.* Let  $s$  be the stereographic projection

$$s(p) = \frac{1}{1 + |p|^2} \begin{pmatrix} 2 \operatorname{Re} p \\ 2 \operatorname{Im} p \\ |p|^2 - 1 \end{pmatrix}.$$

Then its differential is given by

$$d_p s(z) = \operatorname{Re} \left[ \frac{2\bar{z}}{1 + |p|^2} \begin{pmatrix} 1 - p^2 \\ i(1 + p^2) \\ 2p \end{pmatrix} \right]$$



and one finds  $\|d_p s(z)\| = \frac{2|z|}{1+|p|^2}$ . Now given a point  $p$  of an constant angle circle pattern with incident neighboring circle centers  $c_1$  and  $c_2$ . Then  $p$  maps to  $o(p) = s(p)$  on the  $S^2$  and the directions to the vertices of the S-conical Gauss map are given by  $\frac{d_p s(c_i - p)}{\|d_p s(c_i - p)\|}$  (see [BHS06]). The inverse radii of the corresponding spheres can be computed to be

$$R(c_i) = \frac{1 + |c_i|^2 - |c_i - p|^2}{2|c_i - p|}.$$

Thus we find that an edge of the conical minimal net  $f$  is

$$f(c_2) - f(c_1) = \pm \operatorname{Re} \left[ \frac{1}{1 + |p|^2} \left( 2R(c_1) \frac{\bar{c}_2 - \bar{p}}{|c_2 - p|} - 2R(c_2) \frac{\bar{c}_1 - \bar{p}}{|c_1 - p|} \right) \begin{pmatrix} 1 - p^2 \\ i(1 + p^2) \\ 2p \end{pmatrix} \right].$$

In the associated family the diagonals turn by a uniform angle  $\psi$  around  $s(p)$  and by lemma 16 the distance between the diagonals is  $\sin \psi \sin \sigma$  with  $\sigma$  being the circle pattern angle. Therefore we need to add  $i \frac{d_p s(c_1 - p)}{\|d_p s(c_1 - p)\|} \times \frac{d_p s(c_2 - p)}{\|d_p s(c_2 - p)\|}$  (this just becomes  $i s(p)$  in case of orthogonal patterns) and multiply everything with  $e^{i\psi}$  prior to taking the real part for the edge in the associated family. This leaves us with the claimed expression.  $\square$

## 10 Connection to S-Isothermic Nets

When we defined the discrete version of Steiner's formula (4) for Q-nets (definition 4) all that was really required was that the Q-net  $f : V(D) \rightarrow \mathbb{R}^3$  and the normals  $n : V(D) \rightarrow \mathbb{R}^3$  with parallel edges. Instead of requiring  $n$  to have faces tangent to  $S^2$  (as in the conical case) we can ask  $n$  to have edges tangent to  $S^2$  instead. This leads to Koebe polyhedra (see [BHS06]). They can be thought of as half an s-conical Gauss map. Since  $D$  is a quad-graph it is bipartite and we can label the vertices black and white. Removing the white vertices and taking the remaining diagonals as edges leaves us with a net that has the required edges tangent to  $S^2$  and planar faces. It turns out that these nets are Koenigs as well. Remember that in this case we can consider spheres around the vertices of  $n$  that intersect the  $S^2$  orthogonally and that touch at the Koenigs points  $o$ . More general one can define (see for example [BHS06])

*Remark.* The definition of s-isothermic nets we will use here can be considered as a special case of a broader concept by the same name, cf. section 4.4 in [BS08]. Our s-conical surfaces will also fit directly — as a different special case — into this broader concept. The details will not be elaborated here, but in [BH16].

**Definition 14.** An s-isothermic net  $f : V(D) \rightarrow \mathbb{R}^3$  is a Q-net that allows for spheres centered at its vertices such that neighboring spheres touch and the spheres around any face have a common orthogonal circle.

S-isothermic nets are known to be Koenigs nets (see [BS08]).

**Definition 15.** An s-isothermic net  $f : V(D) \rightarrow \mathbb{R}^3$  is called an *s-isothermic minimal net* if it has vanishing mean curvature  $H$  (as in definitions 4 and 5).

**Lemma 25.** *The above definition is equivalent to the definition of  $s$ -isothermic minimal surfaces in [BHS06] (definition 6).*

*Proof.* By means of theorem 5 in [BHS06] being an  $s$ -isothermic minimal surface is equivalent to having a Koebe polyhedron as dual.  $\square$

**Definition 16.** The *black* and *white subnets* of a net  $f$  on  $D$  are the nets  $f_b$  and  $f_w$  obtained by restricting  $f$  to the black and white vertices of  $D$ . Their edges are the diagonals of  $f$  connection vertices of the same respective color.

**Lemma 26.** *Let  $n$  be an  $s$ -conical Gauss map with orthogonally intersecting diagonals, i.e.  $\sigma = \frac{\pi}{2}$ . Then the black and white subnets are Koebe polyhedra.*

*Proof.* Consider the quadrilateral of, say, black diagonals around a white vertex  $n_w$ . The black diagonals intersect the white diagonals through  $n_w$  at their intersection with the sphere around  $n_w$  with radius  $r_w$ ; since they are orthogonal to the white diagonals, they are tangent to this sphere. They are tangent to the unit sphere as well, so they are tangent to the intersection circle of those spheres and form a planar quadrilateral.  $\square$

We want the analog for the dual  $s$ -conical minimal surface  $f$ , but since when dualizing the black diagonals of  $f$  assume the direction of the white ones in  $n$ , the same direct approach does not work. But the associated family comes to the rescue:

**Proposition 27.** *Let  $n$  be an  $s$ -conical Gauss map with orthogonally intersecting diagonals and  $f$  its dual  $s$ -conical minimal surface. Then the black and white subnets of  $f^{\frac{\pi}{2}}$  in the associated family of  $f$  are  $s$ -isothermic minimal nets with dual the same-colored subnet of  $n$ . Their face normals are the opposite-colored subnets of  $n$ .*

*Remark.* Here we make the assumption on the combinatorics of the quad graph on which  $n$  and  $f$  are defined that the black and white subnets are again quad graphs.

*Proof.* W.l.o.g consider the black subnet. By corollaries 22 and 21, the black subnet of  $f^{\frac{\pi}{2}}$  has planar faces whose face normals are  $n_w$ . By the proof of theorem 19, iv), it has spheres around all vertices which touch along the edges. By equation 6, the edges of black quadrilaterals have equal distance to the enclosed white vertex, and by planarity they touch a common circle. The tangent points of the edges with the circle are the touching points of the two spheres on the edge because of corollary 23. Therefore,  $f_b^{\frac{\pi}{2}}$  is an  $s$ -isothermic net.

Now for duality to  $n_b$ , we first assert parallelity of corresponding edges: By corollary 18,ii) and  $\sigma = \psi = \frac{\pi}{2}$ , the edges of  $f_b^{\frac{\pi}{2}}$  are parallel to the white edges of  $f_w$ , each to the one in the same face of  $f$  as itself. So by duality, they are parallel to the black diagonals in the corresponding face of  $n$ , i.e. the corresponding edge of  $n_b$ .

In [BHS06] it was shown that parallel  $s$ -isothermic quadrilaterals whose radii of corresponding spheres are inverse to each other are dual. By theorem 19, iv) and its proof, this is precisely the case since it held for  $\psi = 0$ .  $\square$

The correspondence of the conical and s-isothermic net is not limited to the angles 0 and  $\frac{\pi}{2}$  in the associated family: for s-isothermic minimal nets there is also an associated family, obtained by rotating the edges around the edge normals given by the edge tangent points of the Koebe polyhedron, cf. [BHS06]. The families fit together:

**Theorem 28.** *Let  $n$  be an s-conical Gauss map with orthogonally intersecting diagonals and  $f$  its dual s-conical minimal surface. Then*

$$(f_b^{\frac{\pi}{2}})^\psi = (f^{\frac{\pi}{2}+\psi})_b,$$

*i.e. first taking the black subnet of the  $\frac{\pi}{2}$ -net in the conical associated family and then rotating into the s-isothermic associated family by  $\psi$  is the same as first rotating within the conical associated family to  $\frac{\pi}{2}+\psi$  and then restricting to the black subnet. Analogously for white subnets.*

*Proof.* By proposition 27, the Gauss map of the s-isothermic minimal net  $f_b^{\frac{\pi}{2}}$  is the Koebe polyhedron  $n_b$ . Its edge normals are given by the tangent points of the black diagonals of  $n$  to the unit sphere: but these are exactly the normals  $N$  of the face of the s-conical Gauss map  $n$  containing the diagonal. The edges of  $(f_b^{\frac{\pi}{2}})^\psi$  are the edges of  $f_b^{\frac{\pi}{2}}$  rotated around  $N$  by  $\psi$ . But the edges of  $f_b^{\frac{\pi}{2}}$  are the black diagonals in  $f$  rotated around  $N$  by  $\frac{\pi}{2}$  by corollary 18, ii). So altogether the edges of  $(f_b^{\frac{\pi}{2}})^\psi$  are the black diagonals of  $f$  rotated around  $N$  by  $\frac{\pi}{2} + \psi$ . The edges of  $(f^{\frac{\pi}{2}+\psi})_b$  are the black diagonals of  $f^{\frac{\pi}{2}+\psi}$  which are the black diagonals of  $f$  rotated around  $N$  by  $\frac{\pi}{2} + \psi$  as well. The same works for white instead of black.  $\square$

## A General Conical Minimal Surfaces

The restriction to s-conical nets was necessary for construction via the Koebe machinery, but we can also define general conical minimal surfaces: if we only require our Gauss map to have planar faces tangent to the unit sphere and be a Koenigs net, its dual will still be conical and a minimal surface as in the definition of mean curvature via Steiner's formula.

These surfaces indeed exist, but as of yet we do not know a construction principle other than a geometric evolution from initial data — which is extremely unstable and in practice unsuitable for constructing anything but tiny arbitrary patches of conical minimal surface.

In Figure 19, we depict the construction steps in an example:

- a) In a plane tangent to the unit sphere, choose four vertices.
- b) Any fixed edge determines the adjacent tangent planes; we proceed in one direction.
- c) In the next tangent plane, we again have the freedom to choose two vertices.
- d) Continuing in this way, we construct a strip of quadrangles.

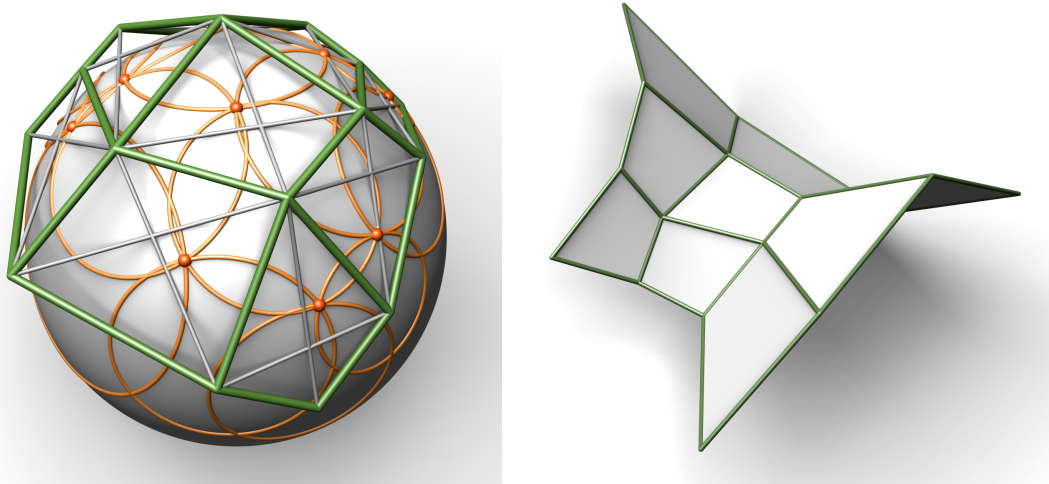


Figure 18: A general conical Gauss map and its dual minimal surface. The faces of the Gauss map touch the unit sphere (at the indicated dots), but the tangent points no longer coincide with the diagonal intersections. The circles of contact of cones and sphere are no longer tangent for diagonally opposite vertices of a face.

- e) Edges along the strip determine new planes, and their intersections the new edge directions.
- f) On two of the edge lines, we can choose the position of the new vertices.
- g) Only now does the Koenigs property come into play: The ratio of diagonal segment lengths determines the position of the vertex on the next edge line uniquely.
- h) This continues until we reach the boundary, where we still have a one-parameter freedom for the edge direction.
- i) Now we have a two-quad-wide strip, and can add new rows in the same way.

## References

- [BH16] A. I. Bobenko and T. Hoffmann, *S-conical cmc surfaces. Towards a unified theory of discrete surfaces with constant mean curvature*, Advances in Discrete Differential Geometry (A. I. Bobenko, ed.), Springer, 2016.
- [BHS06] Alexander I Bobenko, Tim Hoffmann, and Boris A Springborn, *Minimal surfaces from circle patterns: Geometry from combinatorics*, Annals of Mathematics **164** (2006), no. 1, pp. 231–264.

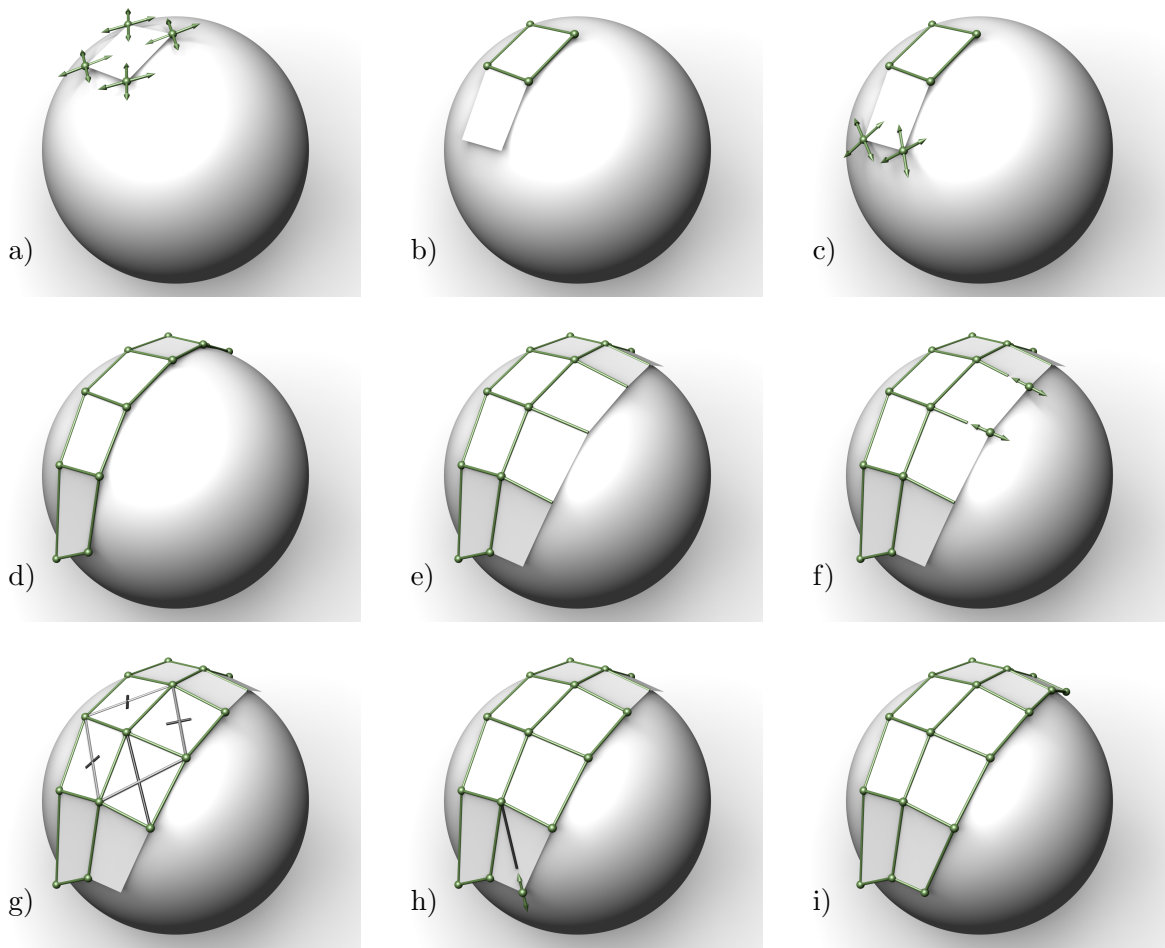


Figure 19: Construction steps for a patch of general conical gauss map

- [BP96] A. Bobenko and U. Pinkall, *Discrete isothermic surfaces*, J. Reine Angew. Math. **475** (1996), 178–208.
- [BP99] A. I. Bobenko and U. Pinkall, *Discretization of surfaces and integrable systems*, Discrete Integrable Geometry and Physics (A. I. Bobenko and R. Seiler, eds.), Clarendon Press, 1999, pp. 3–58.
- [BPW10] A. I. Bobenko, H. Pottmann, and J. Wallner, *A curvature theory for discrete surfaces based on mesh parallelity*, Math. Ann. **348** (2010), 1–24.
- [BS93] G. Brightwell and E. Scheinerman, *Representations of planar graphs*, SIAM Journal on Discrete Mathematics **6** (1993), no. 2, 214–229.

- [BS03] Alexander I. Bobenko and Boris A. Springborn, *Variational principles for circle patterns and Koebe’s theorem*, Trans. Amer. Math. Soc **356** (2003), 659–689.
- [BS08] Alexander I. Bobenko and Yuri B. Suris, *Discrete differential geometry. Integrable structure*, American Mathematical Soc., 2008.
- [BS09] Alexander I. Bobenko and Yuri B. Suris, *Discrete Koenigs nets and discrete isothermic surfaces*, Int. Math. Res. Not. (2009), no. 11, 1976–2012.
- [Ger16] J. D. Gergonne, *Questions proposées/résolues*, Ann. Math. Pure Appl. **7** (1816), 68, 99–100, 156, 143–147.
- [HSFW14] T. Hoffmann, A. O. Sageman-Furnas, and M. Wardetzky, *A discrete parametrized surface theory in  $\mathbb{R}^3$* , arXiv:1412.7293, 2014.
- [Kar89] H. Karcher, *Construction of minimal surfaces*, Rheinische Friedrich-Wilhelms-Universität Bonn, Sonderforschungsbereich 256 Nichtlineare Partielle Differentialgleichungen, Univ., 1989.
- [LPW<sup>+</sup>06] Y. Liu, H. Pottmann, J. Wallner, W. Wang, and Y. Yang, *Geometric modeling with conical meshes and developable surfaces*, ACM Trans. Graphics **25** (2006), no. 3, 681–689.
- [Neo83] E. R. Neovius, *Bestimmung zweier spezieller periodischer Minimalflächen, auf welchen unendlich viele gerade Linien und unendlich viele ebene geodätische Linien liegen*, J. C. Frenckell & Sohn, Helsingfors, 1883.
- [PP93] Ulrich Pinkall and Konrad Polthier, *Computing discrete minimal surfaces and their conjugates*, Experiment. Math. **2** (1993), no. 1, 15–36.
- [Riv96] Igor Rivin, *A characterization of ideal polyhedra in hyperbolic 3-space*, Annals of Mathematics **143** (1996), no. 1, pp. 51–70.
- [Sch90] H. A. Schwarz, *Gesammelte Mathematische Abhandlungen*, vol. 1, Springer-Verlag, Berlin, 1890.
- [Sch92] Oded Schramm, *How to cage an egg*, Inventiones mathematicae **107** (1992), no. 1, 543–560 (English).
- [Sch03] W. K. Schief, *On the unification of classical and novel integrable surfaces. II. Difference geometry*, R. Soc. Lond. Proc. Ser. A Math. Phys. Eng. Sci. **459** (2003), no. 2030, 373–391. MR 1997461 (2004h:39044)
- [Spr05] Boris A. Springborn, *A unique representation of polyhedral types. Centering via Möbius transformations*, Mathematische Zeitschrift **249** (2005), no. 3, 513–517 (English).

- [WYL15] W. Y. Wai Yeung Lam, *Discrete minimal surfaces: critical points of the area functional from integrable systems*, arXiv:1510.08788, 2015.